Stylized Multiresolution Image Representation

Mark Grundland, Chris Gibbs and Neil A. Dodgson

Computer Laboratory
University of Cambridge
Cambridge, United Kingdom

Mark@Eyemaginary.com
http://www.eyemaginary.com/Portfolio/Publications.html

Abstract: We integrate stylized rendering with an efficient multiresolution image representation, enabling a user to control how compression affects the aesthetic appearance of an image. We adopt a point-based rendering approach to progressive image transmission and compression. We use a novel, adaptive farthest point sampling algorithm to represent the image at progressive levels of detail, balancing global coverage with local precision. A progressively generated discrete Voronoi diagram forms the common foundation for our sampling and rendering framework. This framework allows us to extend traditional photorealistic methods of image reconstruction by scattered data interpolation to encompass non-photorealistic rendering. It supports a wide variety of artistic rendering styles based on geometric subdivision or parametric procedural textures. Genetic programming enables the user to create original rendering styles through interactive evolution by aesthetic selection. We compare our results with conventional compression and we discuss the implications of using non-photorealistic representations for highly compressed imagery.

Categories and Subject Descriptors (according to ACM CCS)**:** I.3.3 [Computer Graphics]: Picture/Image Generation; I.4.10 [Image Processing and Computer Vision]: Image Representation.

Keywords: Non-photorealistic rendering, multiresolution image representation, progressive image compression, point based rendering, farthest point image sampling, Voronoi diagram, Delaunay triangulation, genetic programming, design of graphical styles, digital art.

ADDITIONAL ILLUSTRATIONS

August, 2006

Original image sources:
Waterloo Brag Zone [http://links.uwaterloo.ca/bragzone.base.html]
FreeFoto.Com [http://www.freefoto.com/]

Table of Illustrations

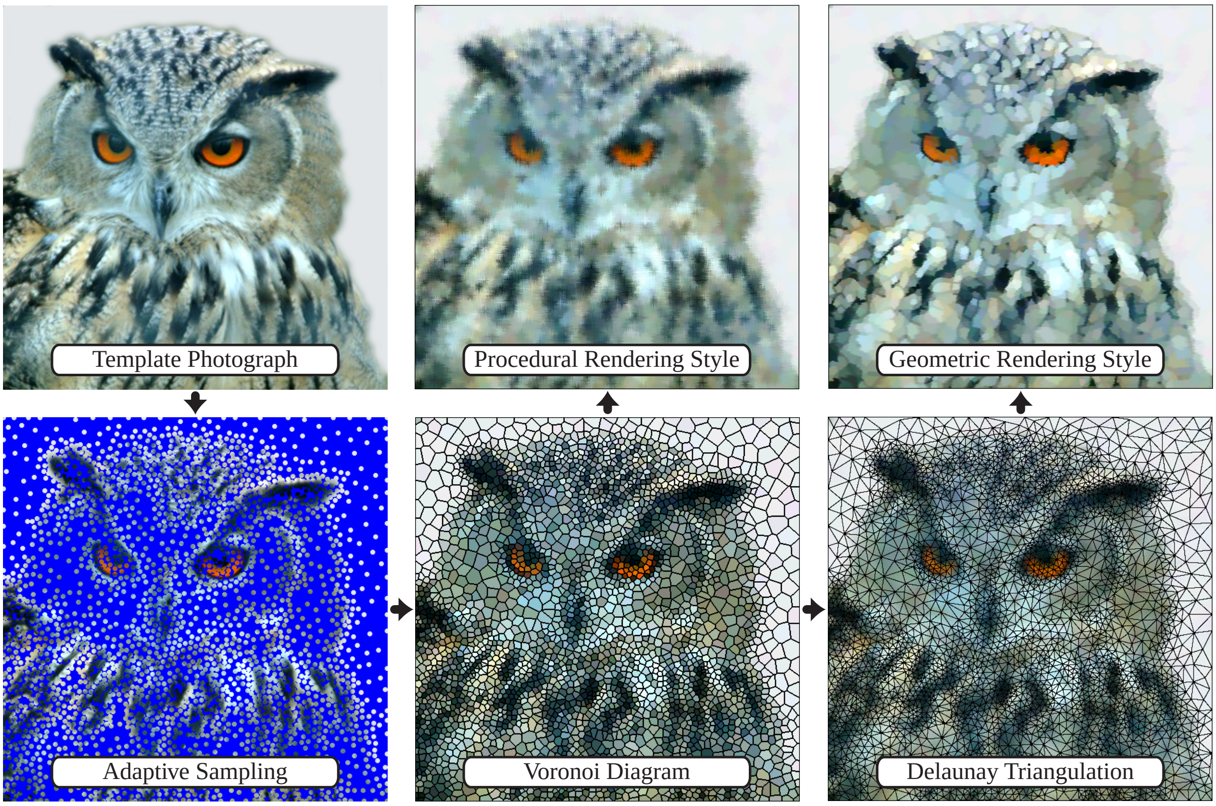

Figure 1: Our image rendering process using coverage adaptive sampling (3200 samples ≈ 2%).

Figure 2: Test images:
"Lena" (512 × 512) and "Park" (512 × 512),
"Autumn" (400 × 400) and "Cambridge" (400 × 400).

Template image (250 × 250)

Farthest point sampling (3125 samples ≈ 5%)

Voronoi diagram

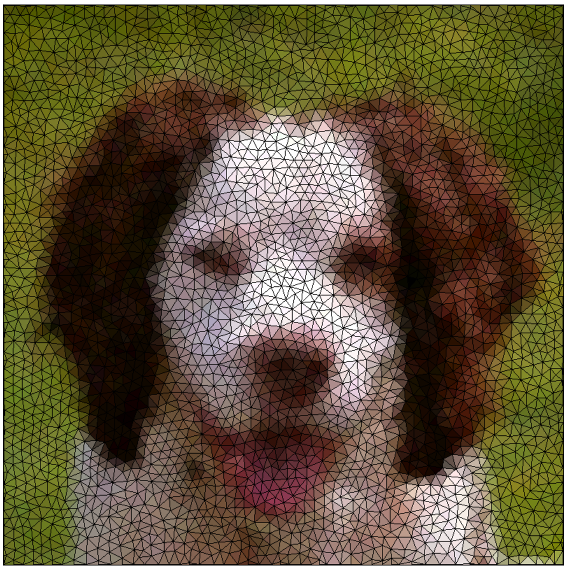

Delaunay triangulation

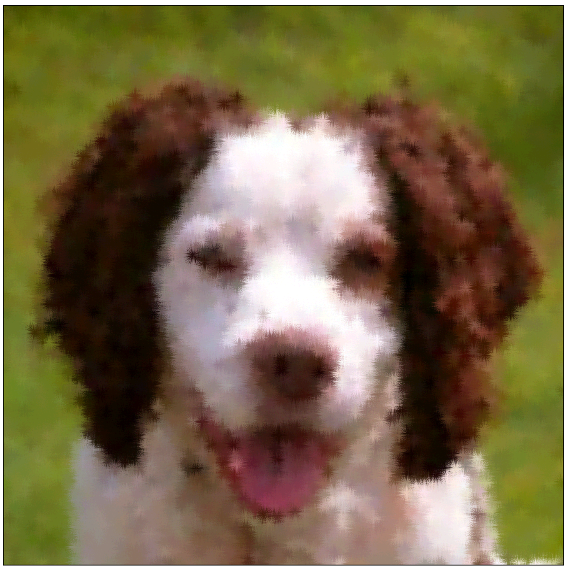

"Chalk painting" procedural rendering style

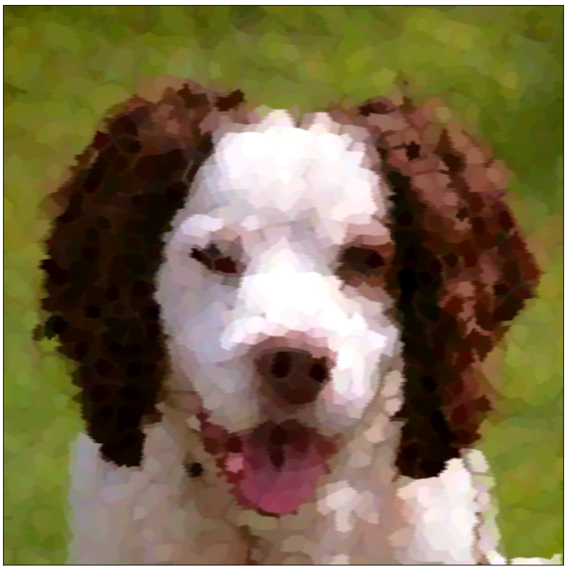

"Paint strokes" geometric rendering style

Figure 3: Spatial partitions used in our image rendering process.

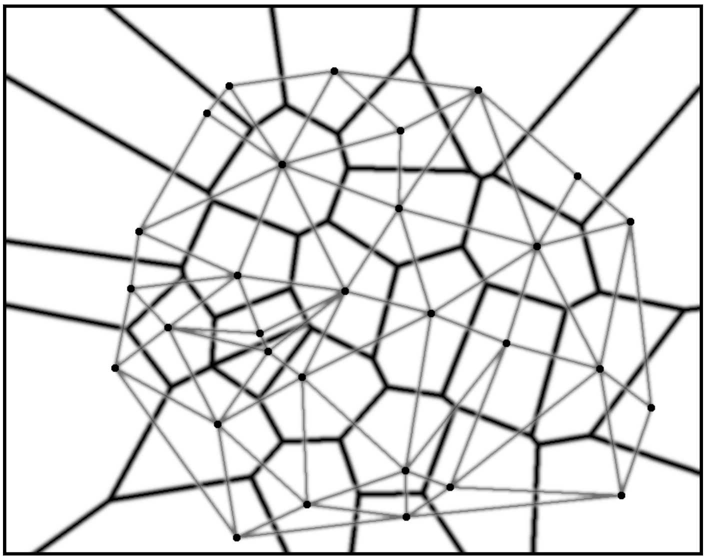

Figure 4: Spatial partitions: Voronoi diagram (black), Delaunay triangulation (gray), and sample sites (dot).

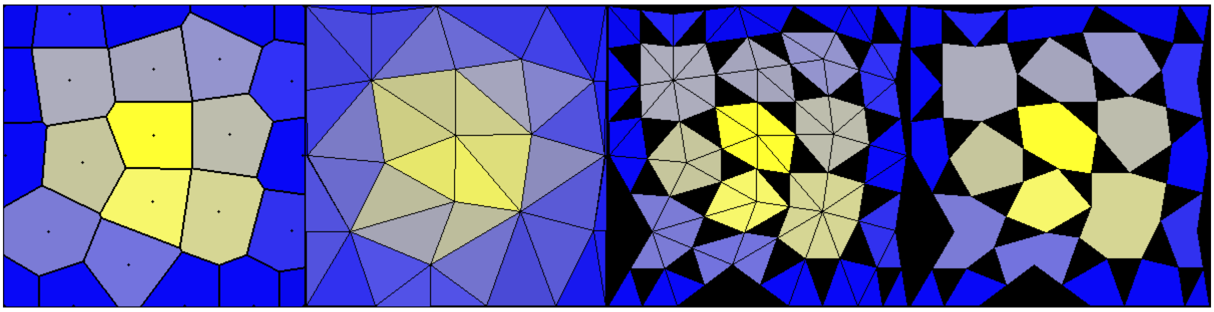

Voronoi polygons | Delaunay triangles | Delaunay stars | Mosaic tiles

Figure 5: Visualizing the spatial configuration of sample sites.

Sampling Strategies	Accurate Reconstruction	Progressive Refinement	Uniform Coverage	Isotropic Distribution	Blue Noise Spectrum	Centroidal Regions	Heterogeneous Configurations
Periodic	★★★★	★	★★★★	★	★	★★★★	★
Non-Periodic	★★★	★★★★	★★★	★	★	★★★	★★
Farthest Point	★★★★	★★★★	★★★★	★★★	★★★★	★★★	★★
Jittered	★	★	★★	★★★	★★★	★★	★★★
Quasirandom	★★	★★★	★★	★★	★★	★★	★★★
Random	★	★★	★	★★★★	★	★	★★★★

★★★★ Superior ★★★ Good ★★ Fair ★ Poor

Figure 6: Qualitative evaluation of non-adaptive sampling.

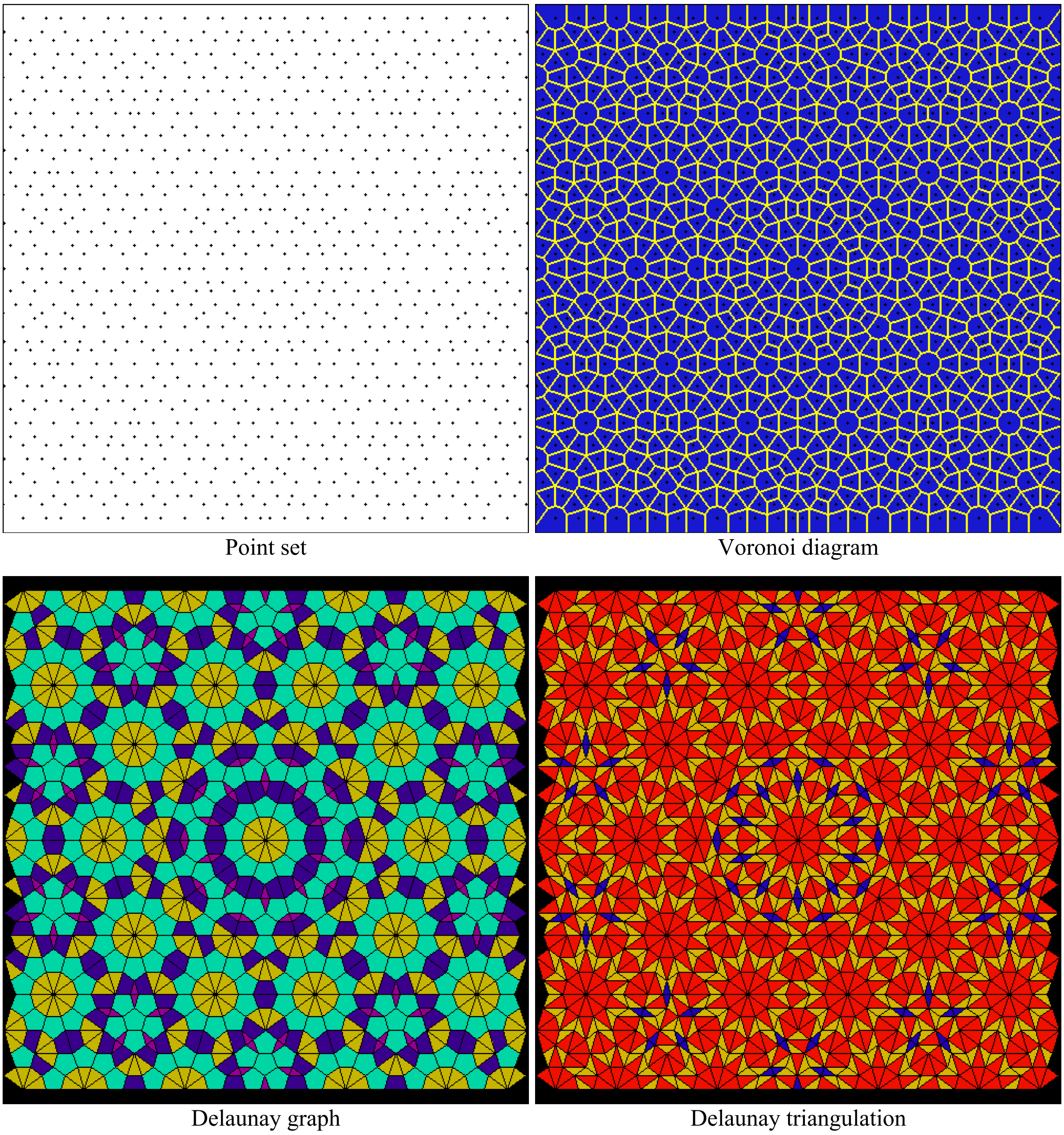

Figure 7: Non-periodic tilings by spatial partitions. A non-periodic, rotationally symmetric point set (top left) is depicted as a planar tiling induced by a Voronoi diagram (top right), a Delaunay graph (bottom left), and a Delaunay triangulation (bottom right). This set of 1035 points comprises a cut-and-project quasicrystal derived from the usual root lattice of the H_2 non-crystallographic Coxeter group.

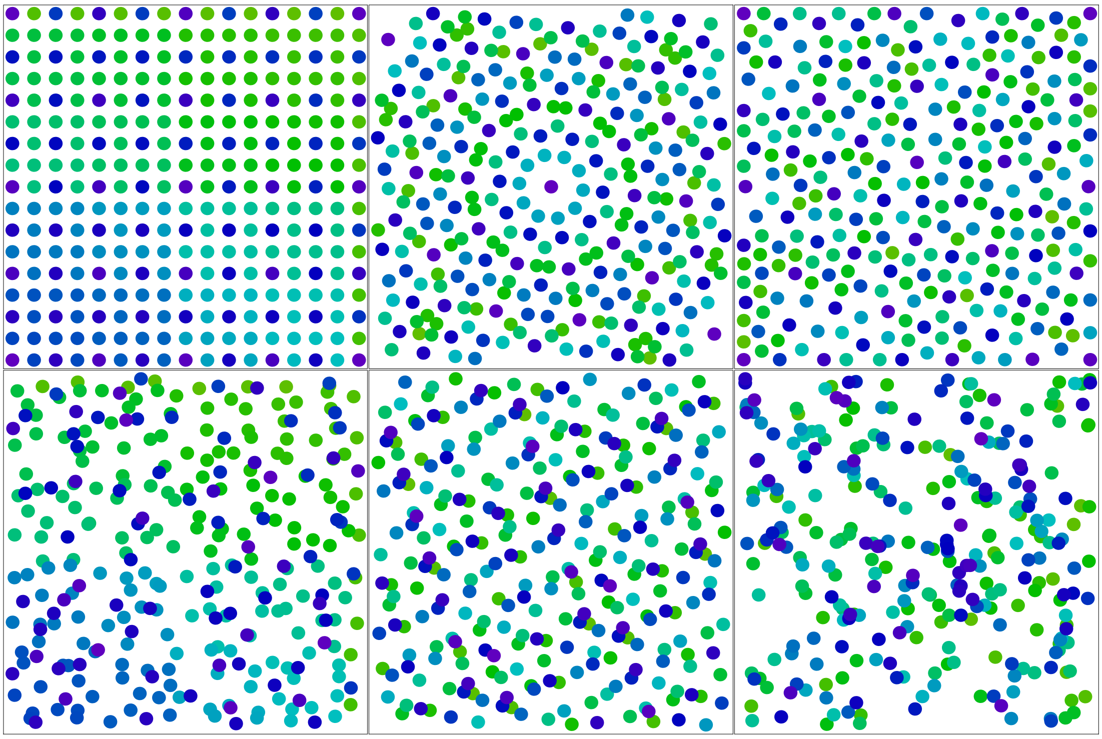

Figure 8: Non-adaptive sampling strategies: periodic sampling (top left), non-periodic sampling (top center), farthest point sampling (top right), jittered sampling (bottom left), quasirandom sampling (bottom center), random sampling (bottom right). The sampling sequences start with the blue sites and finish with the green sites.

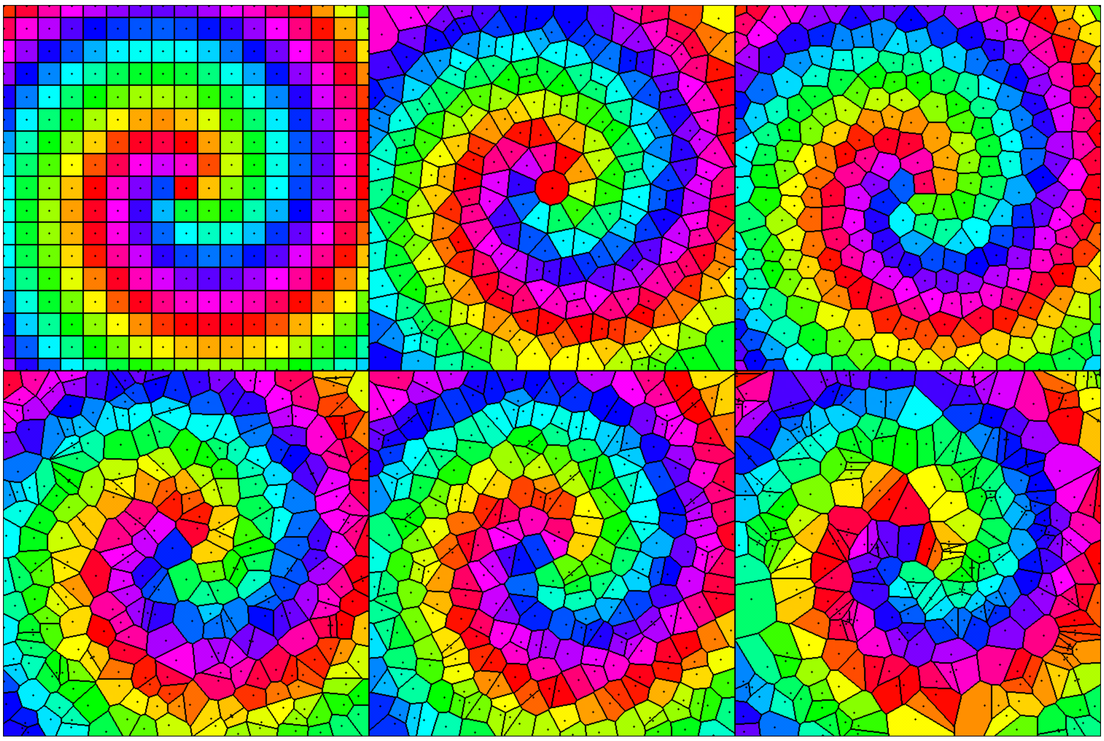

Figure 9: Voronoi diagrams of non-adaptive sampling strategies applied to a color spiral test image: periodic sampling (top left), non-periodic sampling (top center), farthest point sampling (top right), jittered sampling (bottom left), quasirandom sampling (bottom center), random sampling (bottom right).

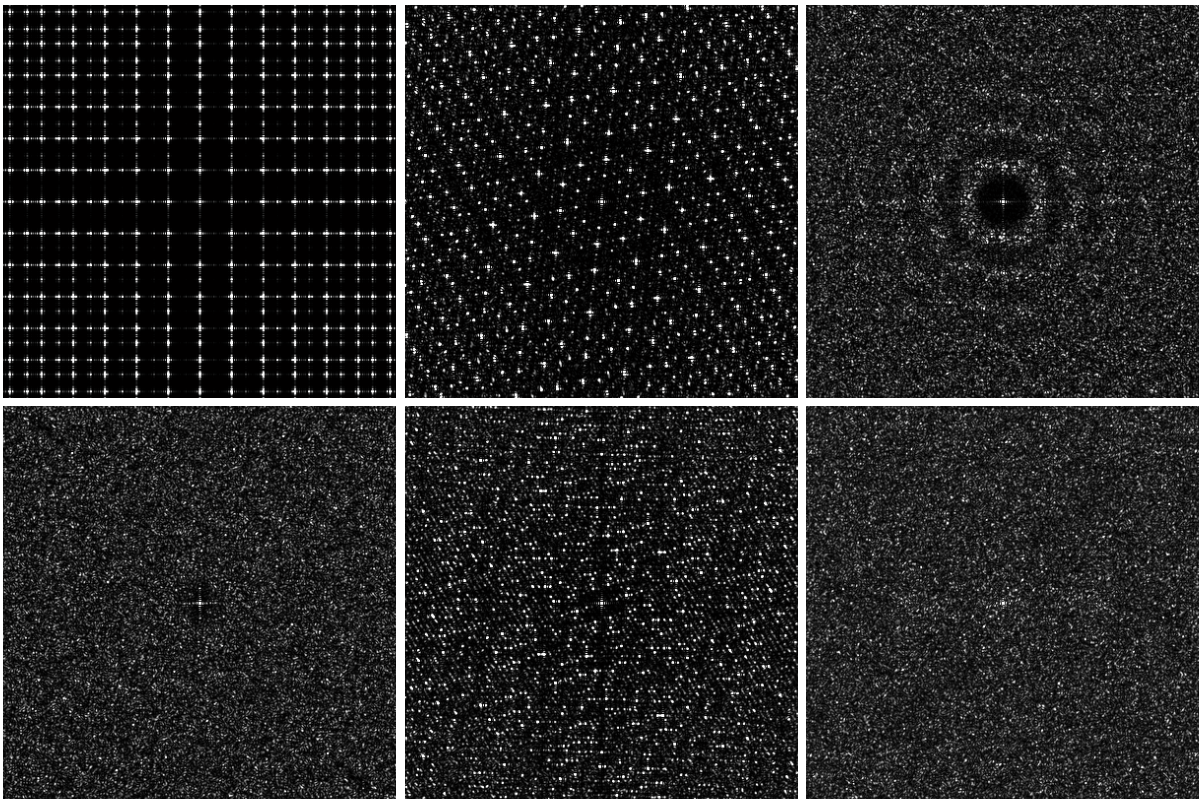

Figure 10: Fourier power spectrums of non-adaptive sampling strategies: periodic sampling (top left), non-periodic sampling (top center), farthest point sampling (top right), jittered sampling (bottom left), quasirandom sampling (bottom center), random sampling (bottom right).

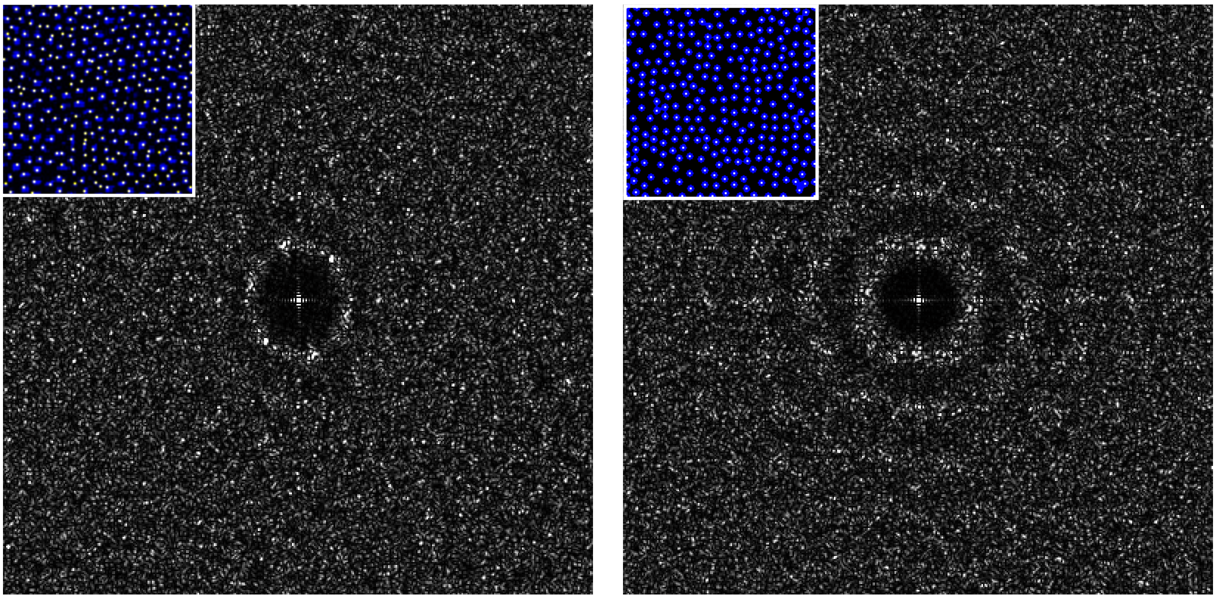

Cone photoreceptors in the human eye
Sample sites reflect the layout of cone cells
(eye scan [Klassen, 2000] by A. Roorda & D. Williams)

Farthest point sampling
Sample sites reflect a packing of circular disks
(generated algorithmically [Eldar, et al., 1997])

Figure 11: Blue noise Fourier power spectrums.

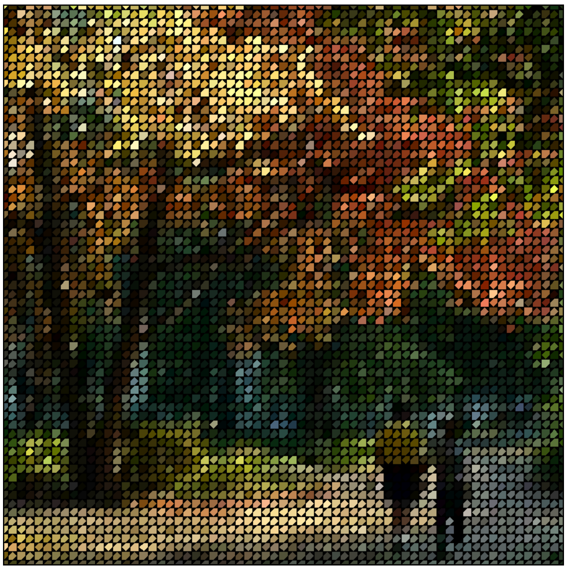
Periodic sampling

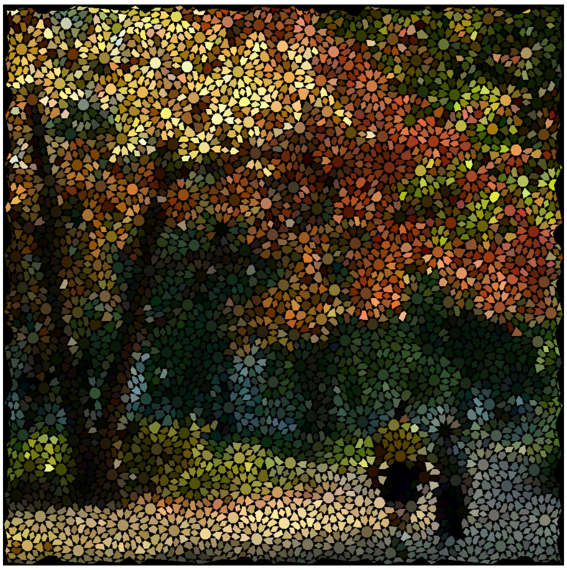
Nonperiodic sampling

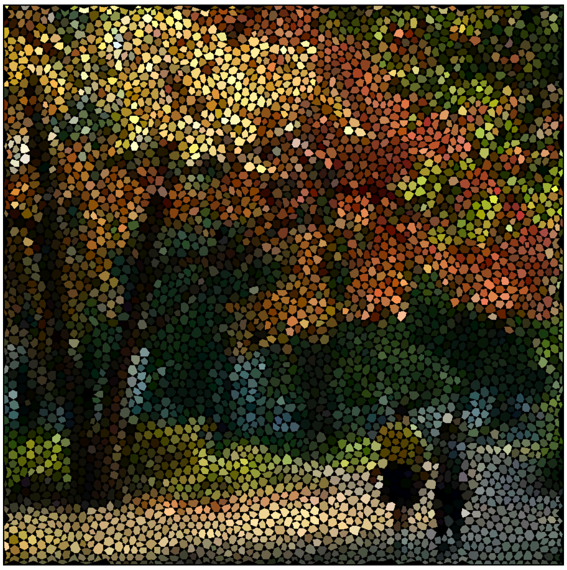
Farthest point sampling

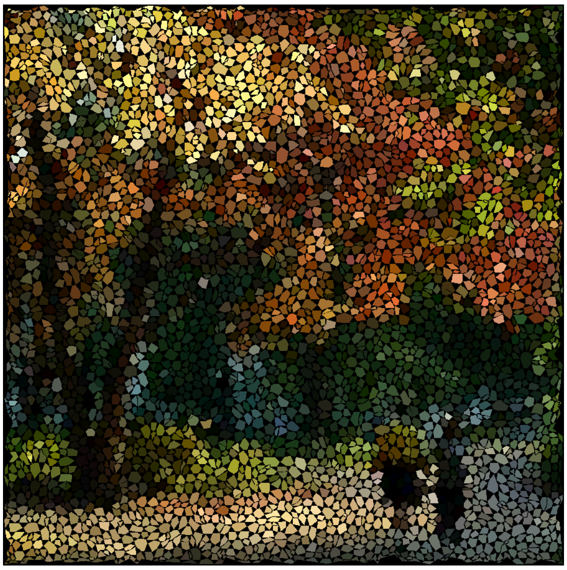
Jittered sampling

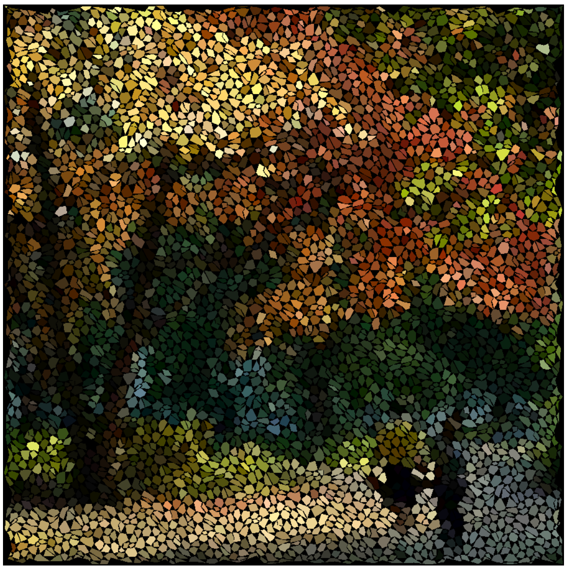
Quasirandom sampling

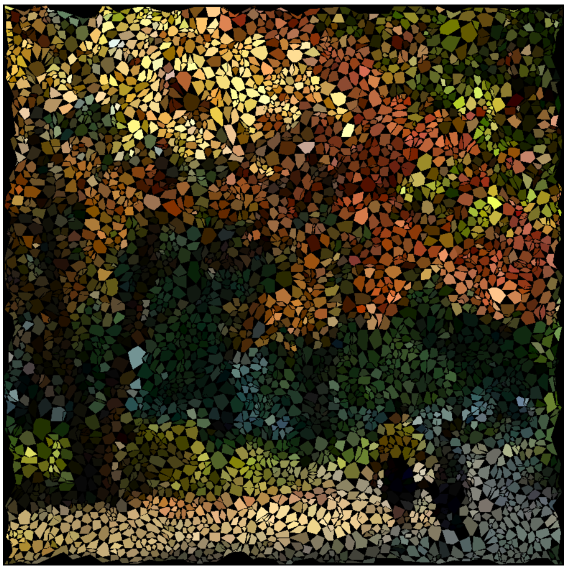
Random sampling

Figure 12: Non-adaptive sampling rendered using the “mosaic” style (4225 samples ≈ 2.6%).

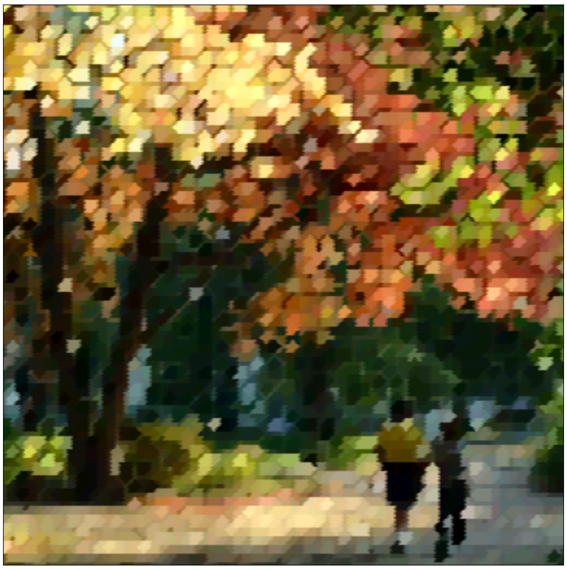

Periodic sampling

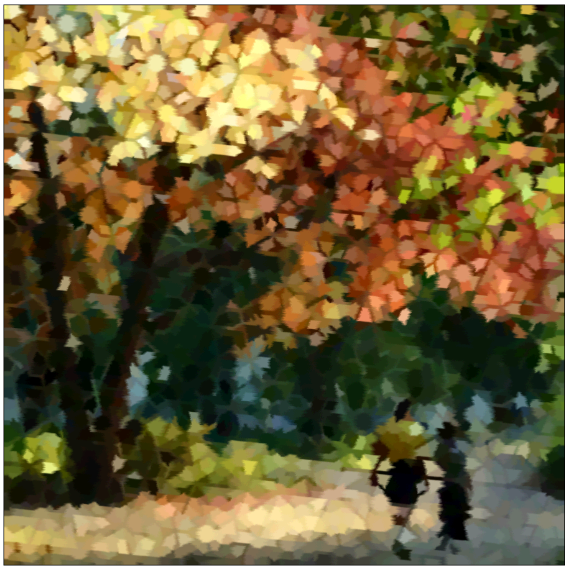

Nonperiodic sampling

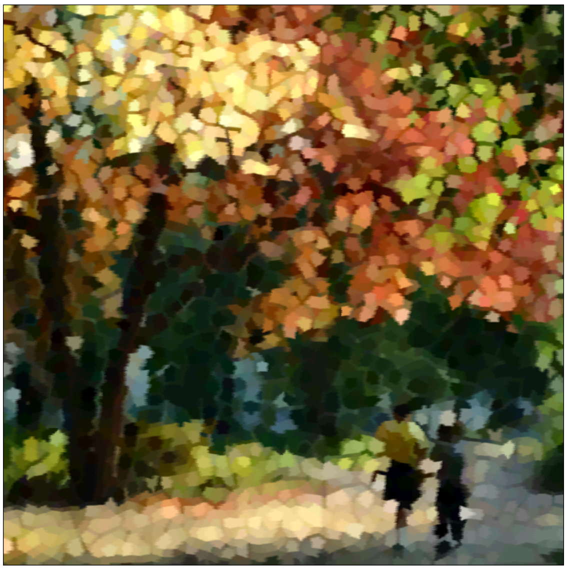

Farthest point sampling

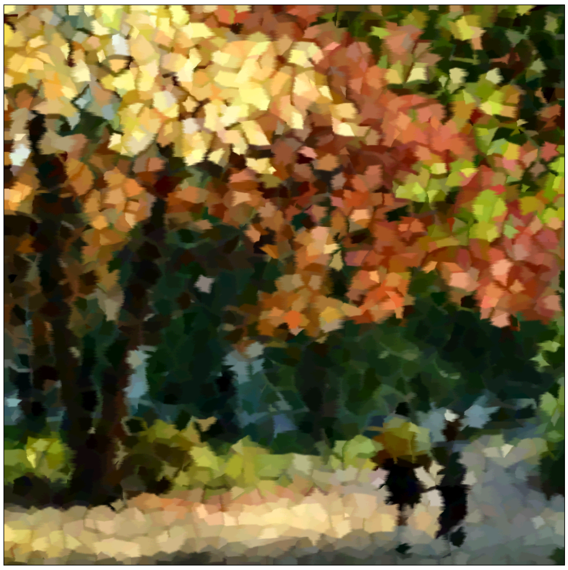

Jittered sampling

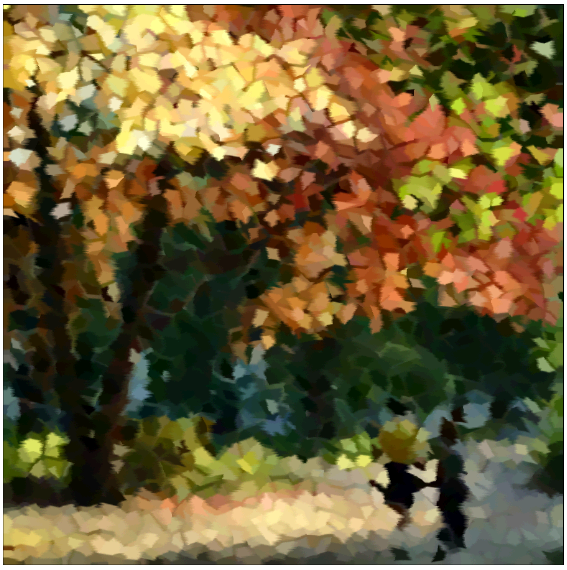

Quasirandom sampling

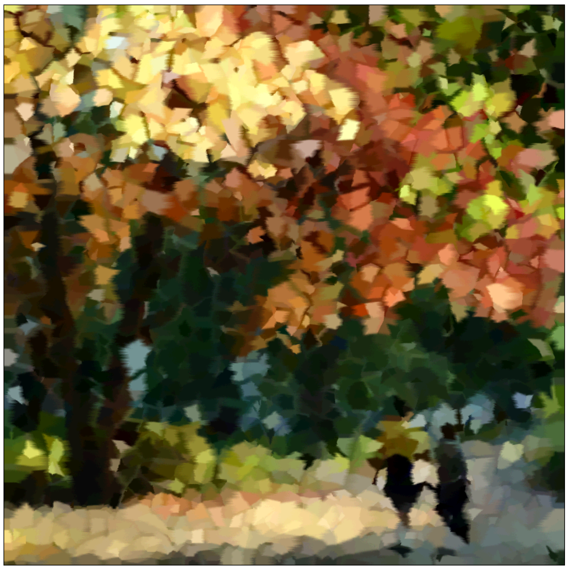

Random sampling

Figure 13: Non-adaptive sampling rendered using the “paint strokes” style (4225 samples ≈ 2.6%).


Periodic sampling

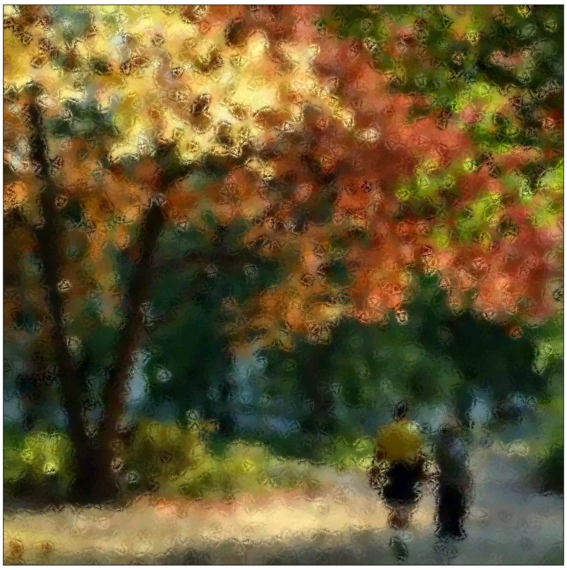
Nonperiodic sampling

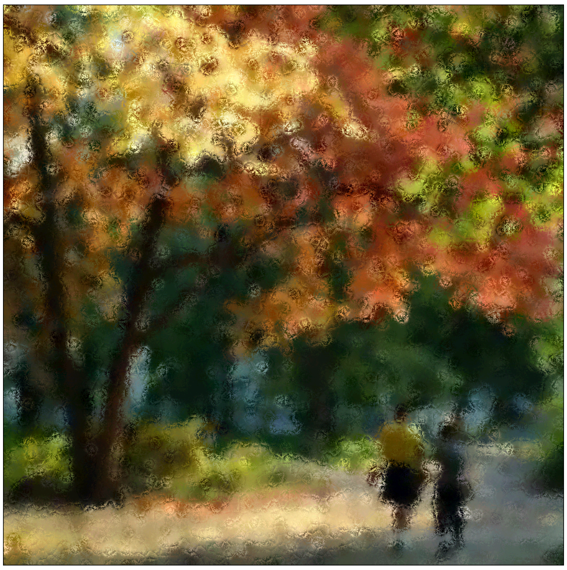
Farthest point sampling

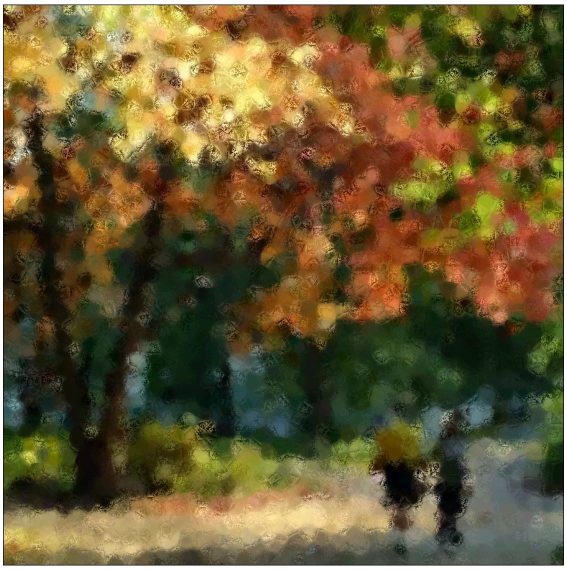
Jittered sampling

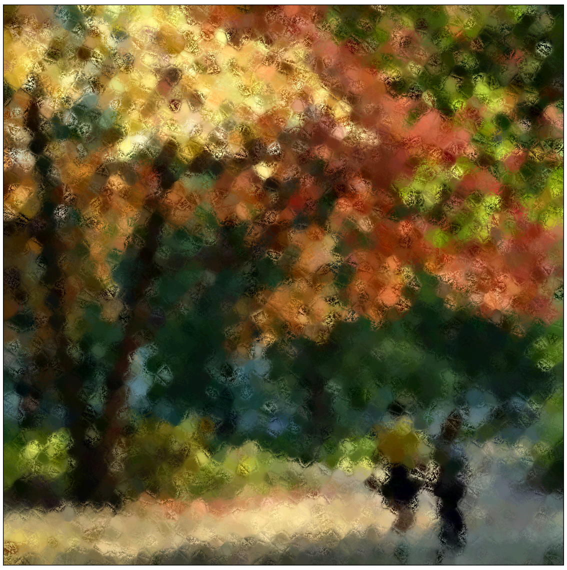
Quasirandom sampling

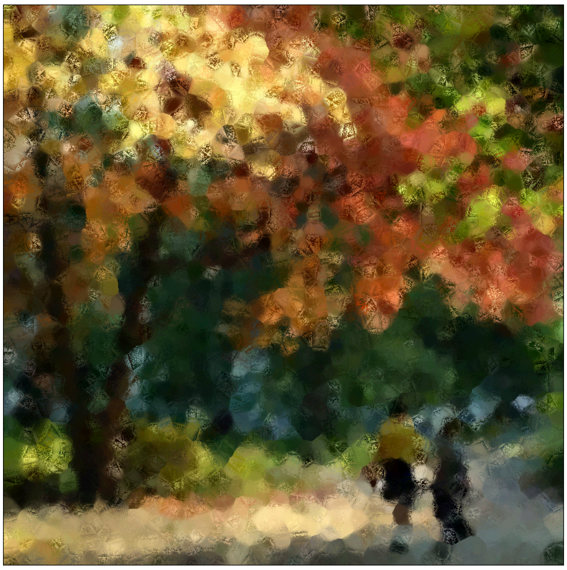
Random sampling

Figure 14: Non-adaptive sampling rendered using the “sponge painting” style (4225 samples ≈ 2.6%).

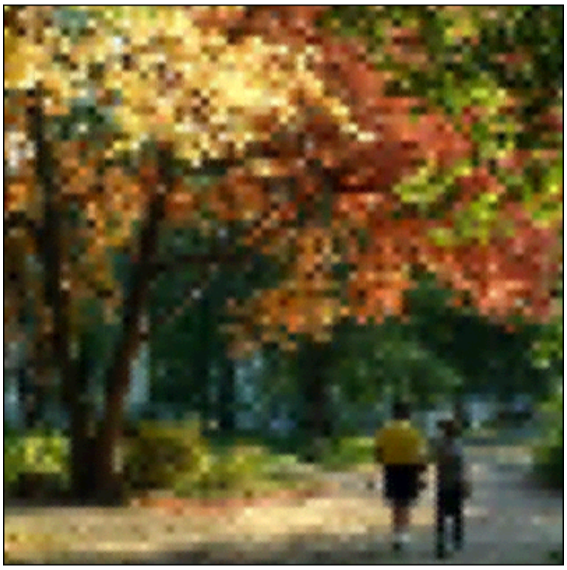

Periodic sampling (PSNR = 18.58)

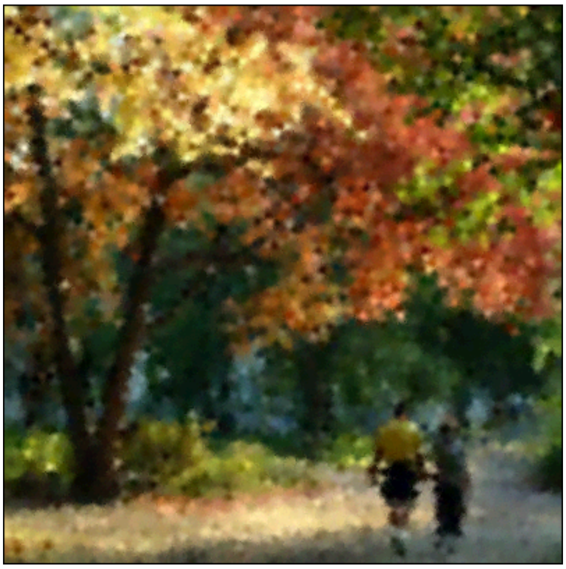

Nonperiodic sampling (PSNR = 18.52)

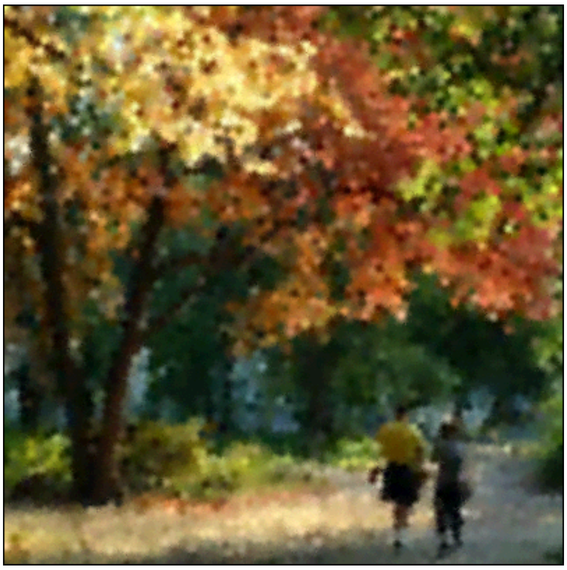

Farthest point sampling (PSNR = 18.55)

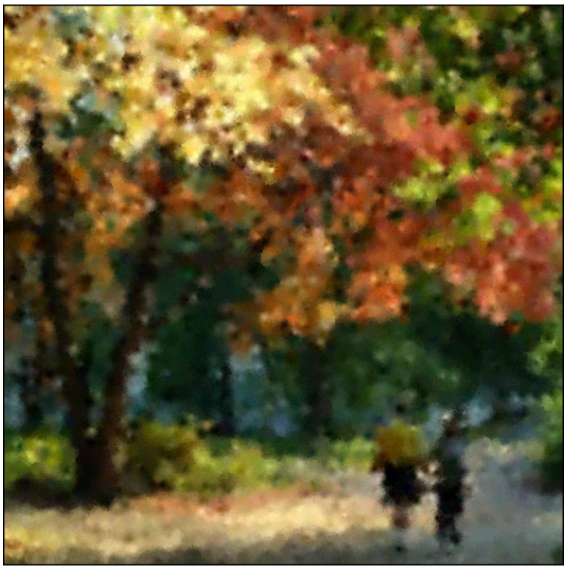

Jittered sampling (PSNR = 18.31)

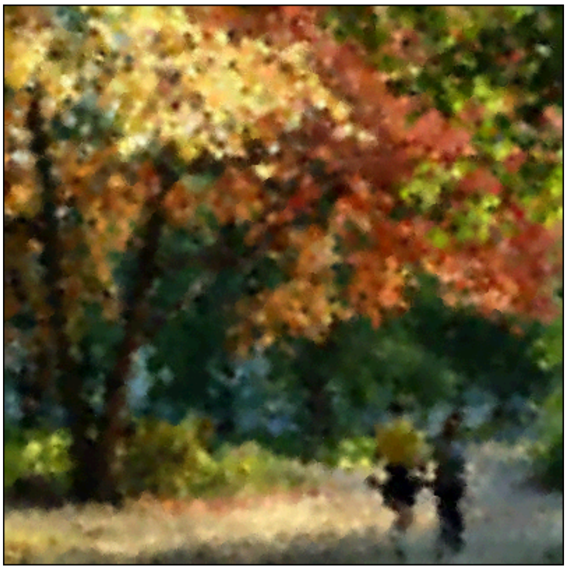

Quasirandom sampling (PSNR = 18.24)

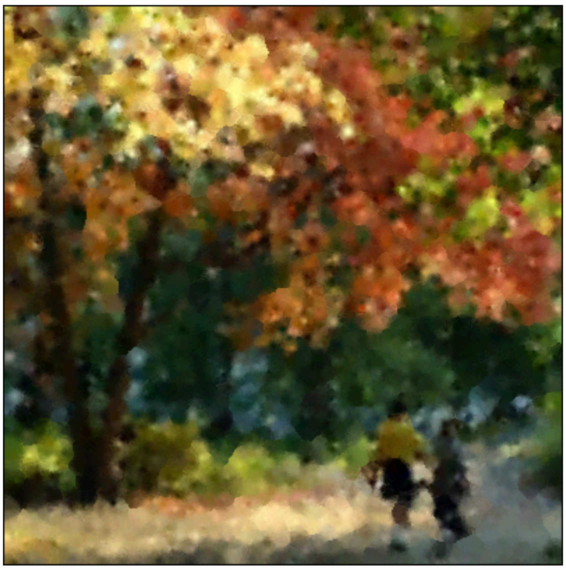

Random sampling (PSNR = 17.93)

Figure 15: Non-adaptive sampling rendered using Shepard interpolation (4225 samples ≈ 2.6%).

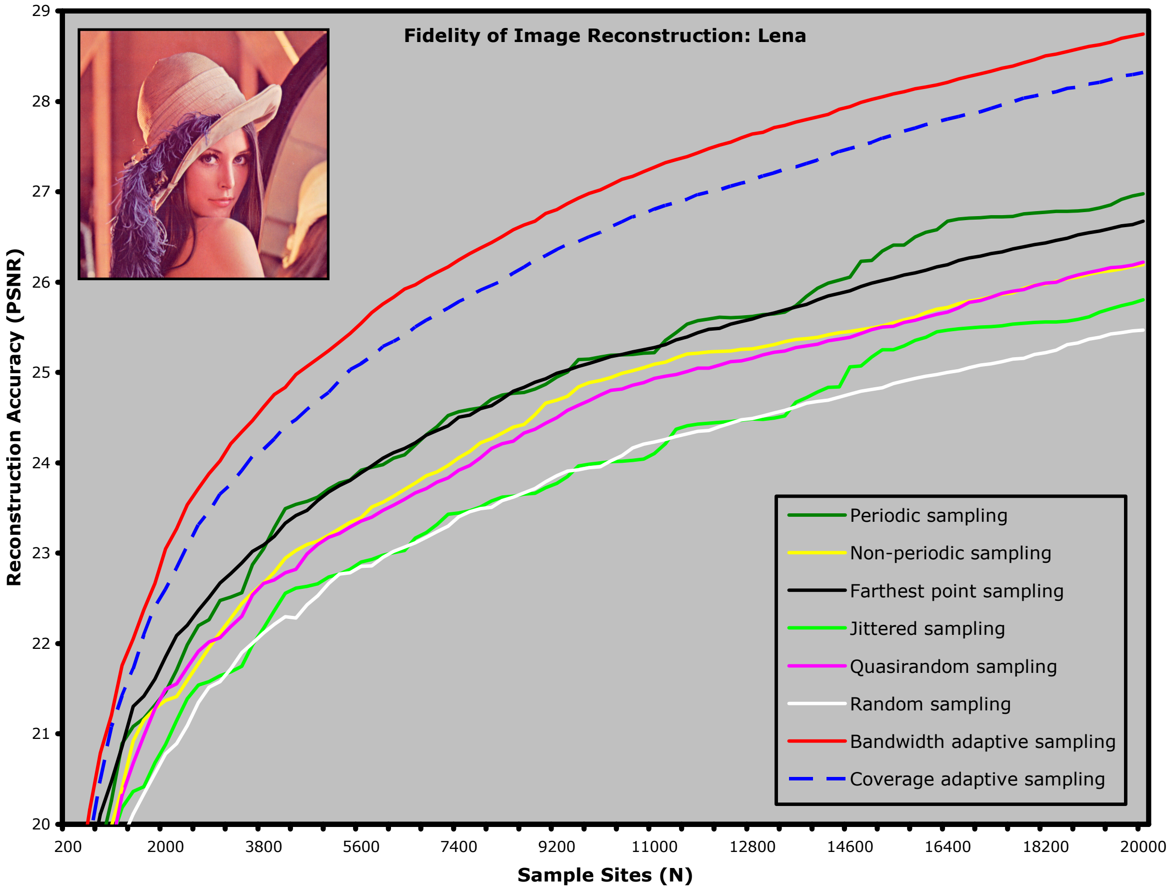

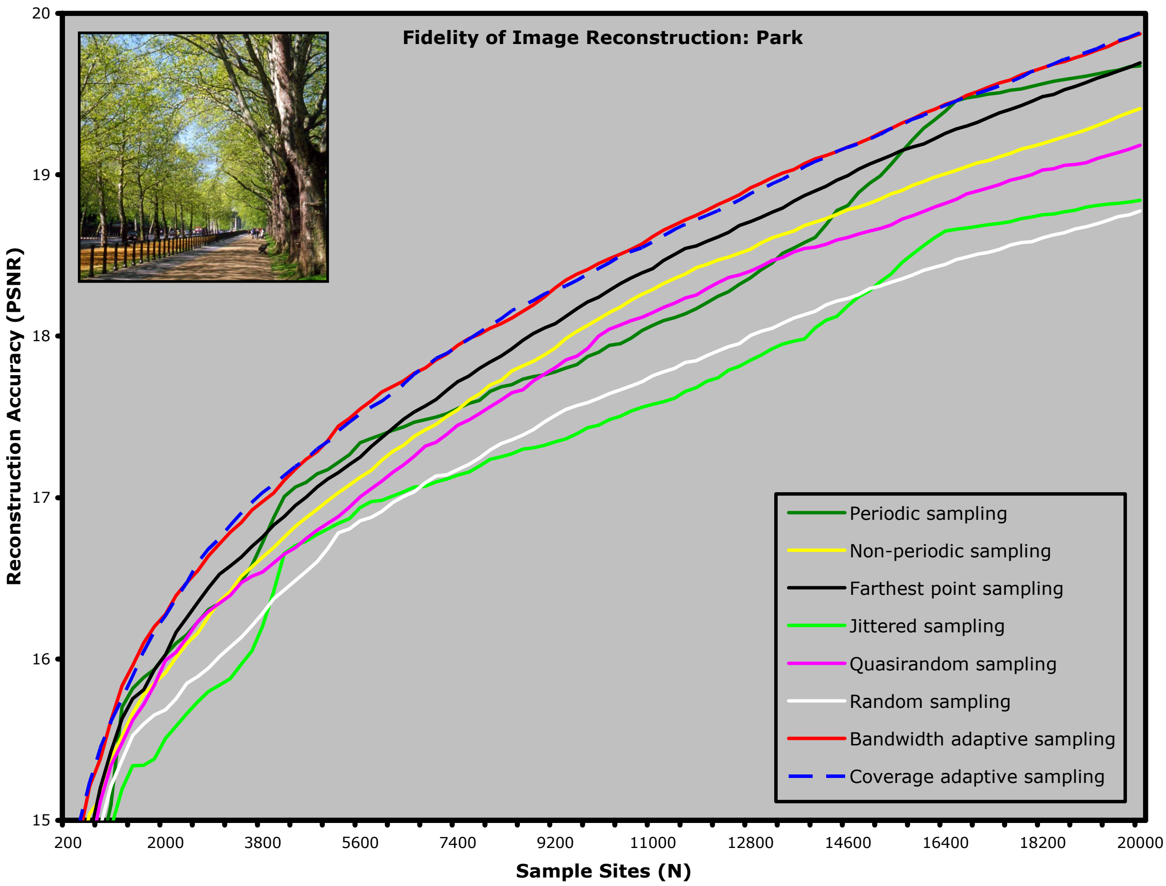

Figure 16: Quantitative evaluation of non-adaptive and adaptive sampling rendered using Gouraud shading.

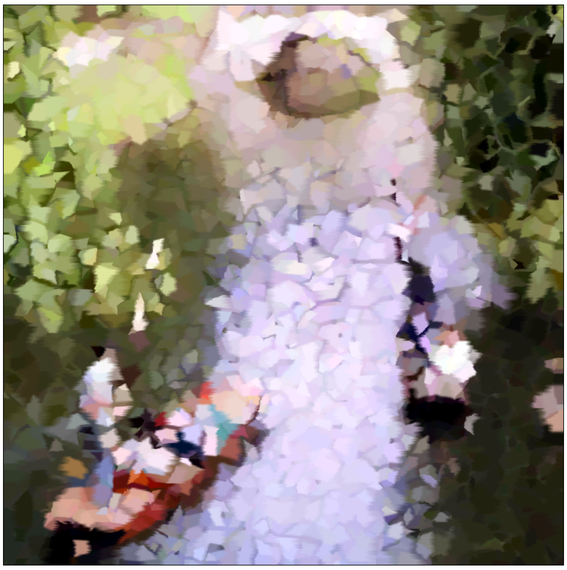

Random sampling

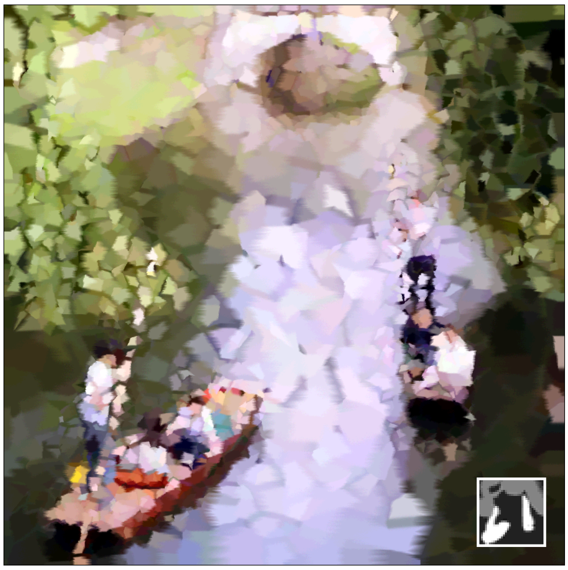

Rejection sampling using random sampling

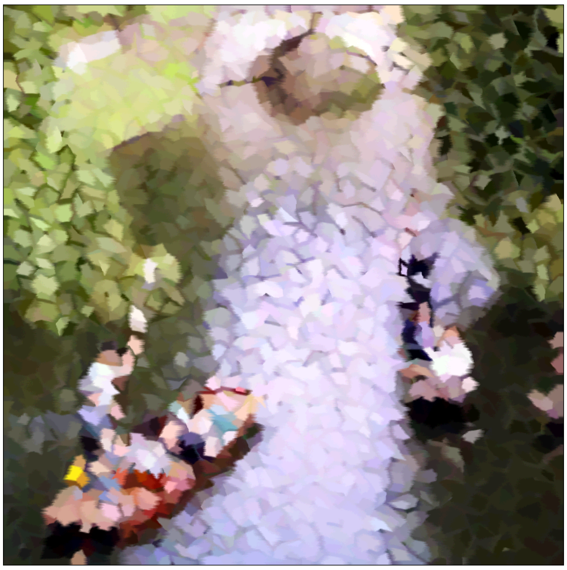

Quasirandom sampling

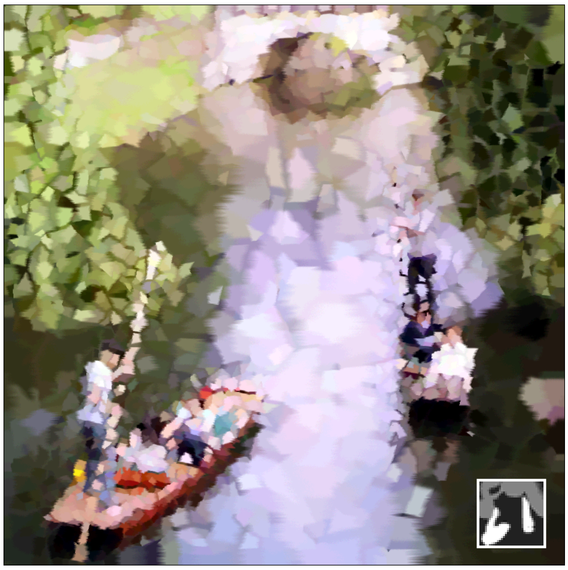

Rejection sampling using quasirandom sampling

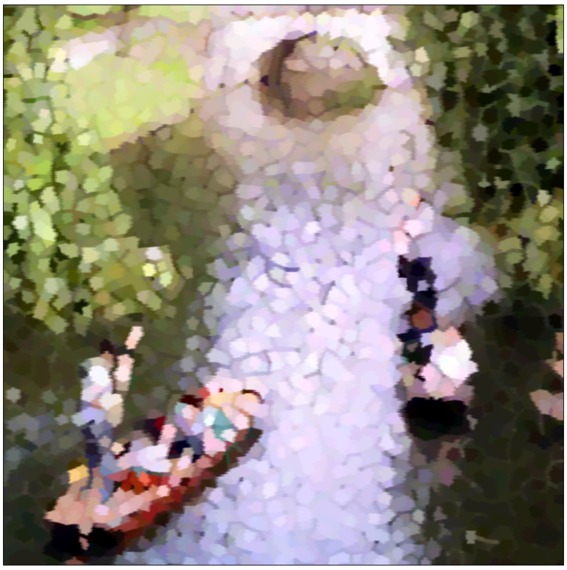

Farthest point sampling

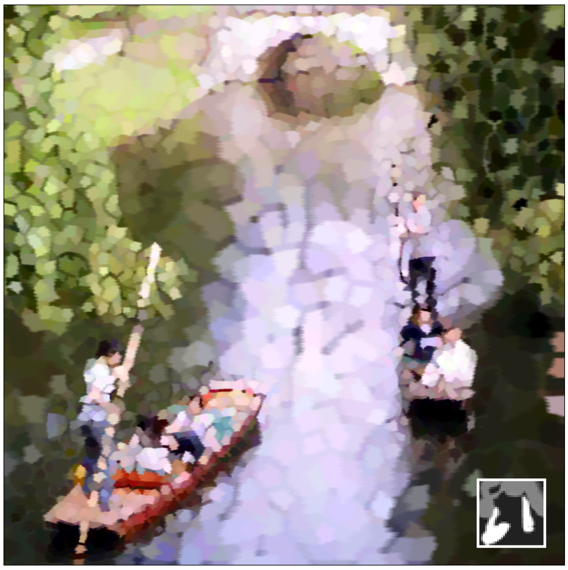

Importance driven farthest point sampling

Figure 17: Importance sampling rendered using the “paint strokes” style (4000 samples ≈ 2.5%).

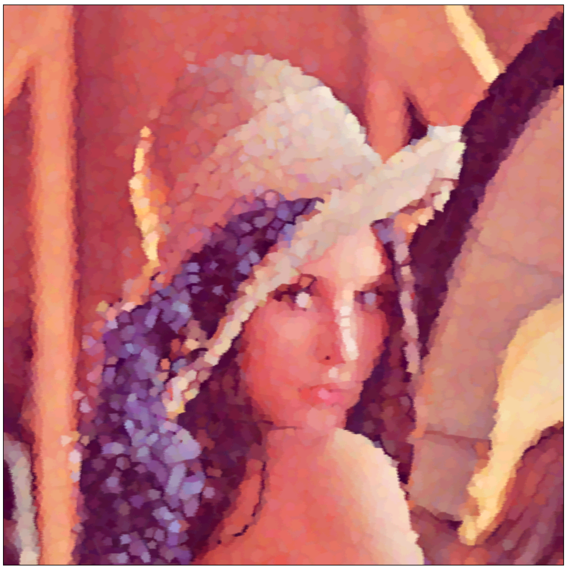
Farthest point sampling

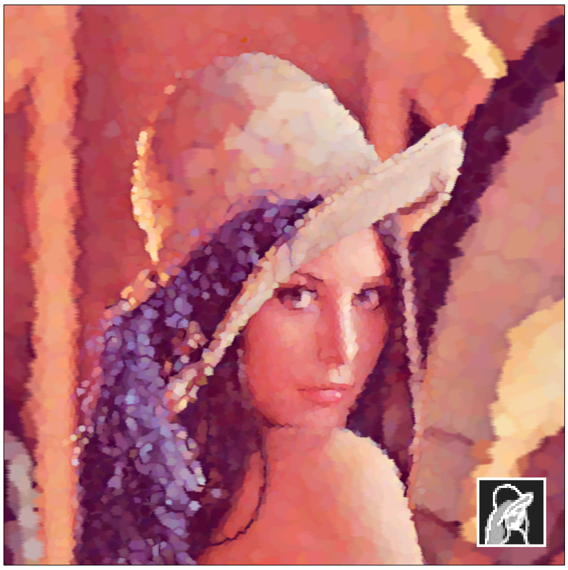
Importance driven farthest point sampling

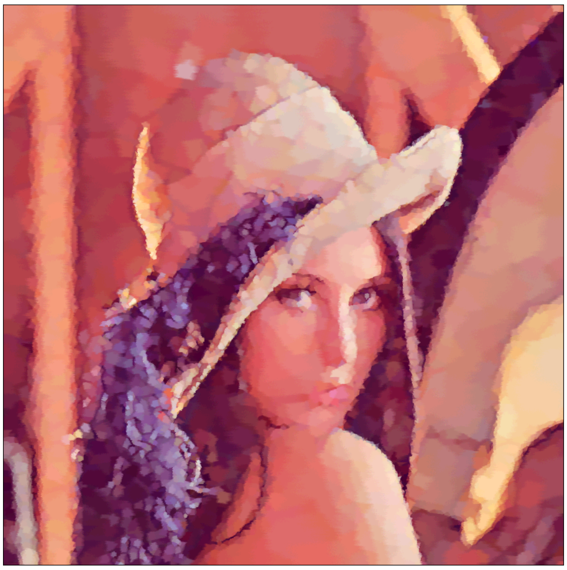
Bandwidth adaptive sampling

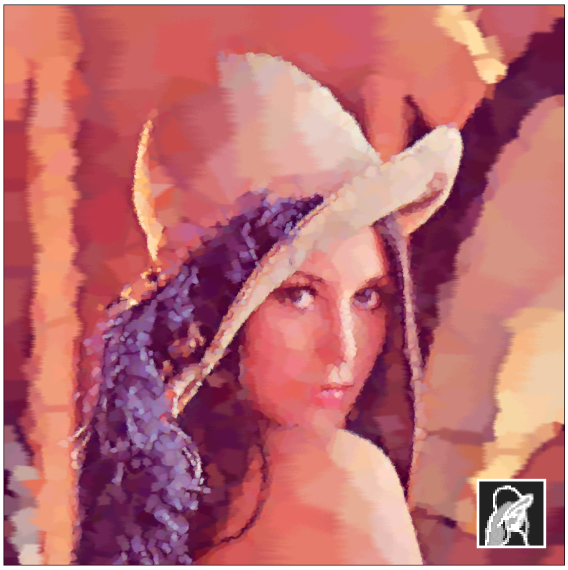
Importance driven bandwidth adaptive sampling

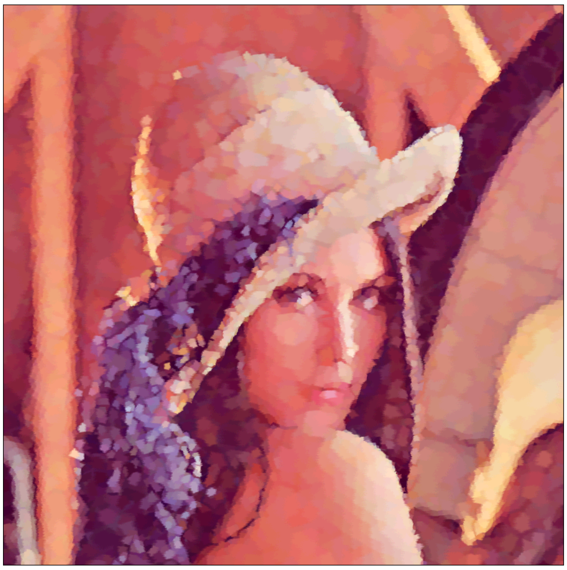
Coverage adaptive sampling

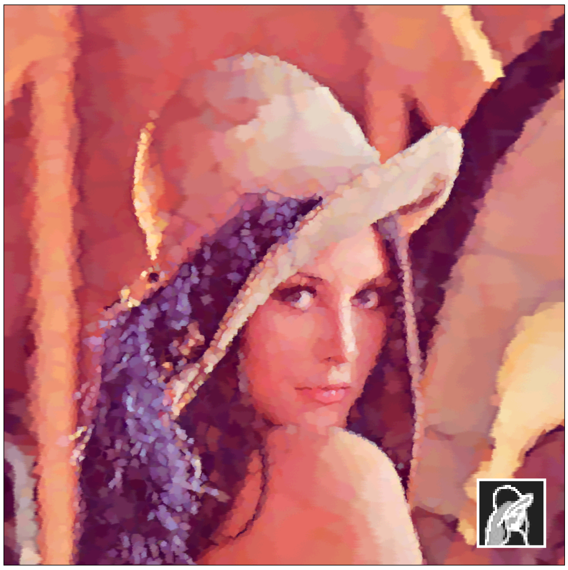
Importance driven coverage adaptive sampling

Figure 18: Importance driven adaptive sampling rendered using the “paint strokes” style (6554 samples ≈ 2.5%).

Farthest point sampling (PSNR = 25.22)

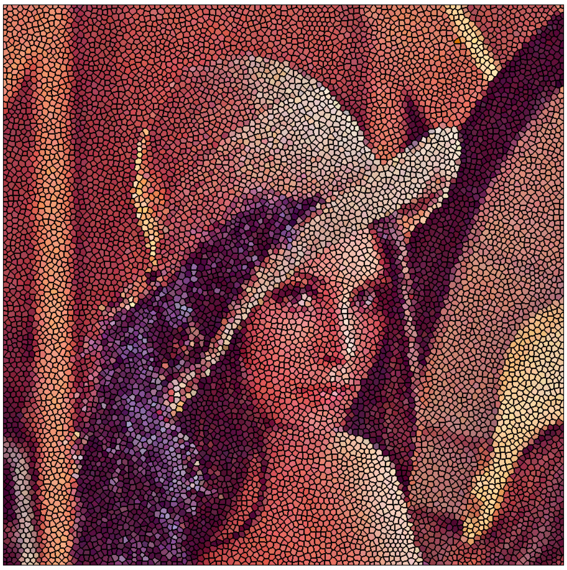

Farthest point sampling

Bandwidth adaptive sampling (PSNR = 27.11)

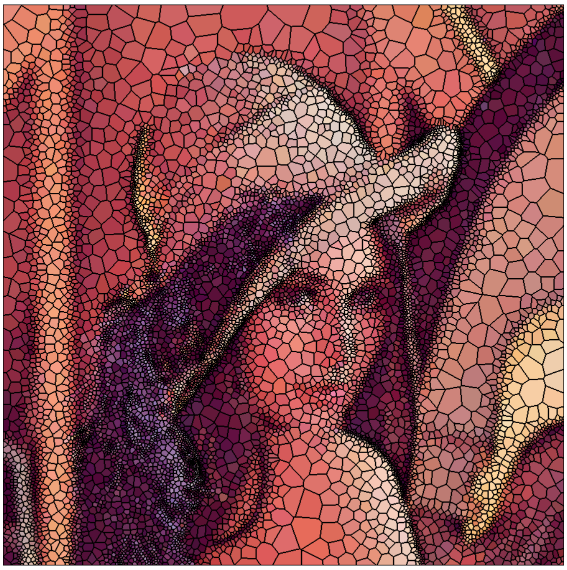

Bandwidth adaptive sampling

Coverage adaptive sampling (PSNR = 26.70)

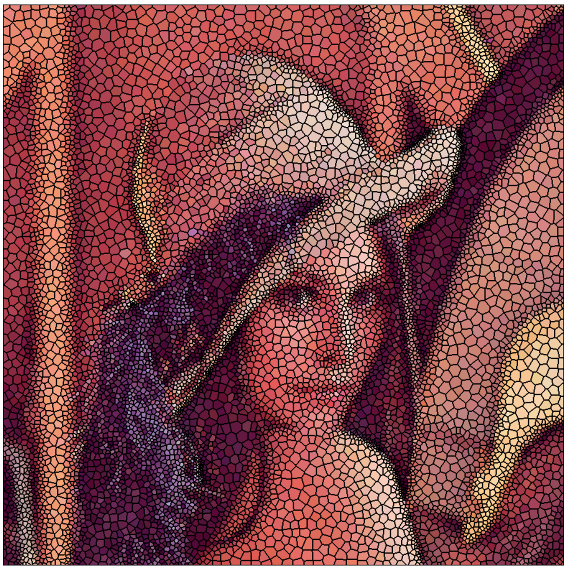

Coverage adaptive sampling

Figure 19: Adaptive sampling rendered using Gouraud shading and Voronoi diagrams (10485 samples ≈ 4%).

“Balloons” (350 × 350)

Farthest point 6% sampling

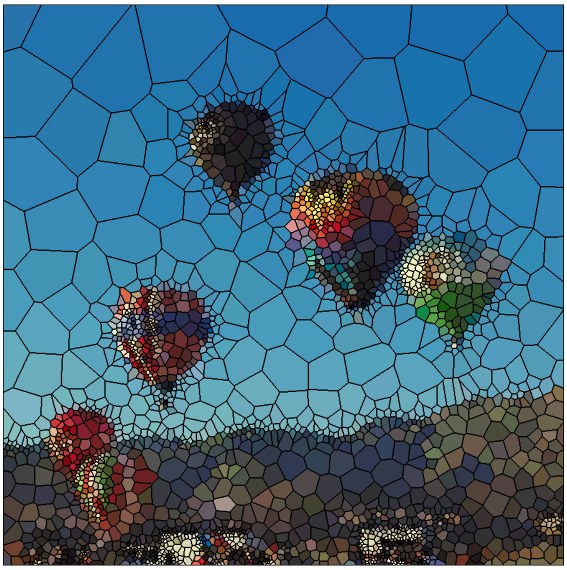

Bandwidth adaptive 2% sampling

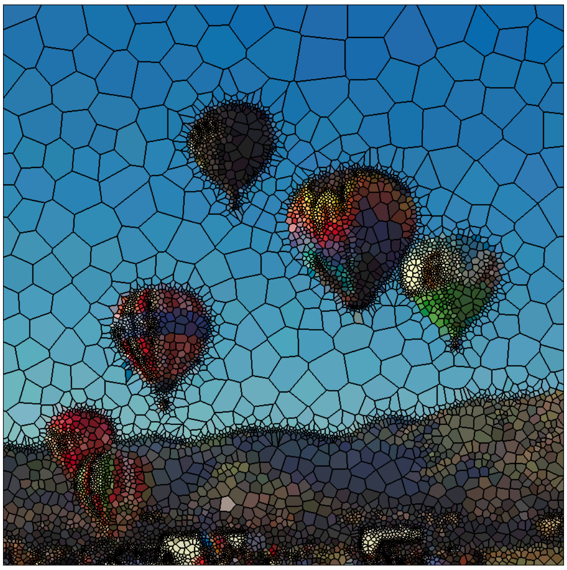

Bandwidth adaptive 6% sampling

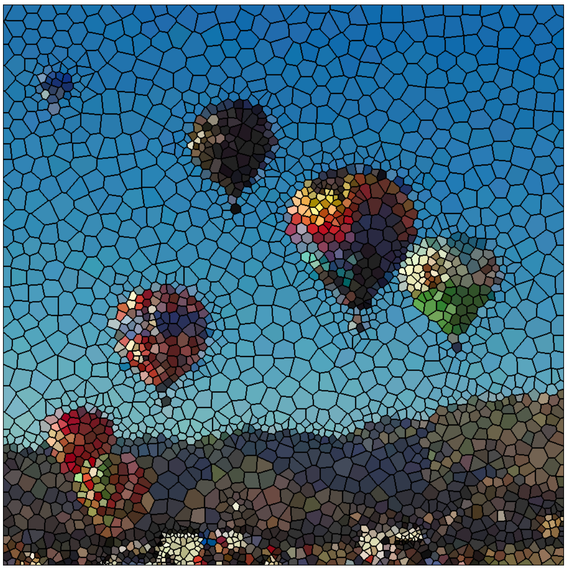

Coverage adaptive 2% sampling

Coverage adaptive 6% sampling

Figure 20: Adaptive sampling rendered using Voronoi diagrams.

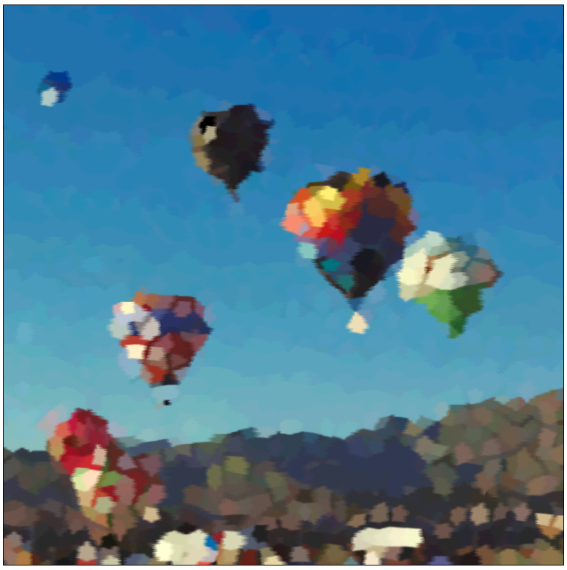

Farthest point 2% sampling

Farthest point 6% sampling

Bandwidth adaptive 2% sampling

Bandwidth adaptive 6% sampling

Coverage adaptive 2% sampling

Coverage adaptive 6% sampling

Figure 21: Adaptive sampling rendered using the “paint strokes” style.

Farthest point 2% sampling (PSNR = 22.32)

Farthest point 6% sampling (PSNR = 24.04)

Bandwidth adaptive 2% sampling (PSNR = 24.31)

Bandwidth adaptive 6% sampling (PSNR = 26.58)

Coverage adaptive 2% sampling (PSNR = 23.54)

Coverage adaptive 6% sampling (PSNR = 26.06)

Figure 22: Adaptive sampling rendered using Gouraud shading.

Voronoi polygons filled with
the color of their sample sites (PSNR = 18.02)

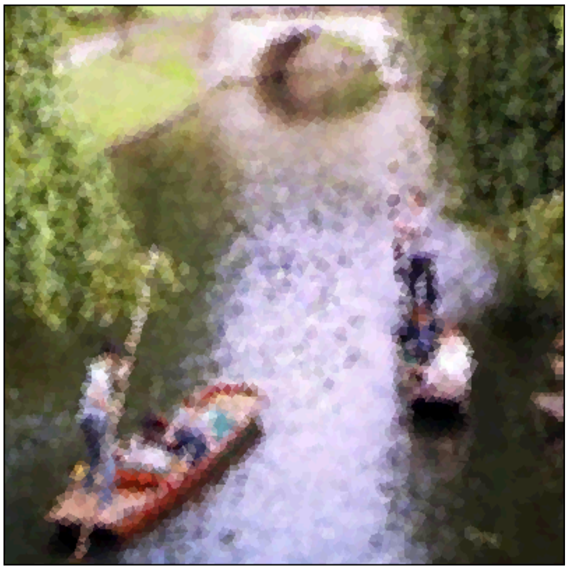

Delaunay triangles filled with
the mean color of their vertices (PSNR = 19.08)

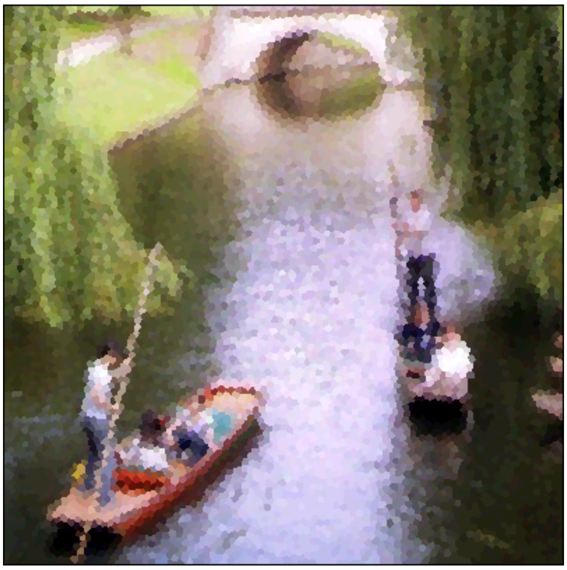

Voronoi polygons filled with
the mean color of their image region (PSNR = 20.17)

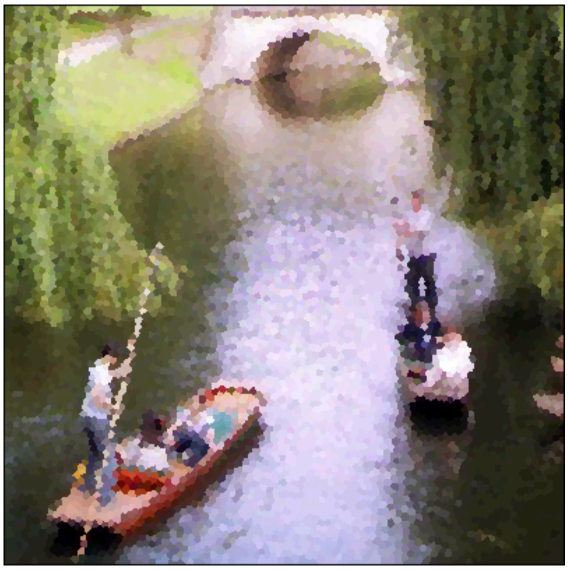

Voronoi polygons filled with
the median color of their image region (PSNR = 19.86)

Figure 23: Coloring Voronoi and Delaunay spatial partitions using farthest point sampling (8000 samples ≈ 5%).

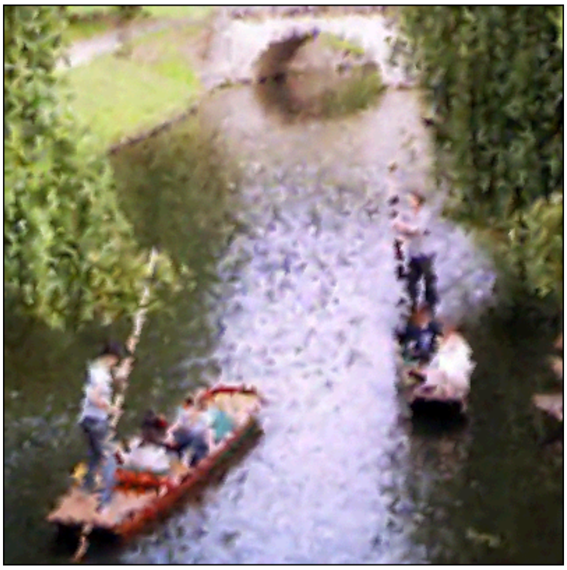

Standard Gouraud shading of Delaunay triangles uses linear interpolation of mesh edges (PSNR = 19.37)

"Brush marks" geometric rendering style uses nonlinear interpolation of mesh edges (PSNR = 19.00)

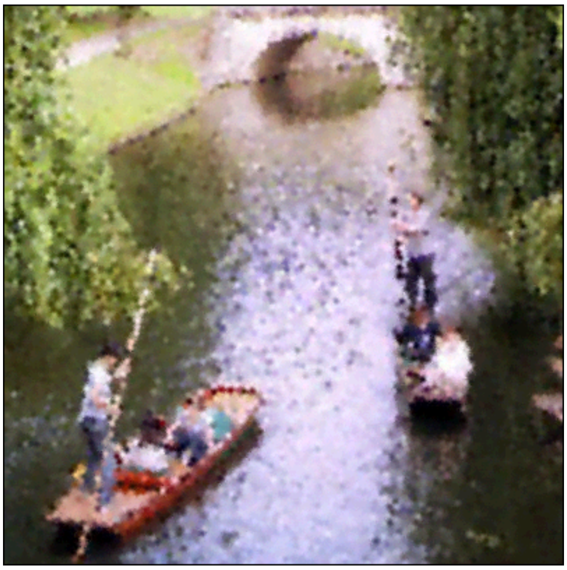

Standard Shepard interpolation of Voronoi polygons relies on squared Euclidean distance (PSNR = 19.47)

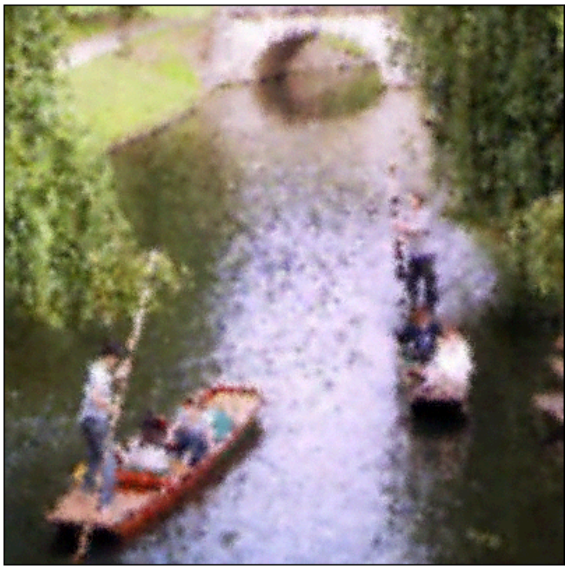

"Soft touch" procedural rendering style relies on normal Euclidean distance (PSNR = 19.61)

Figure 24: Variants of Gouraud and Shepard interpolation using farthest point sampling (8000 samples ≈ 5%).

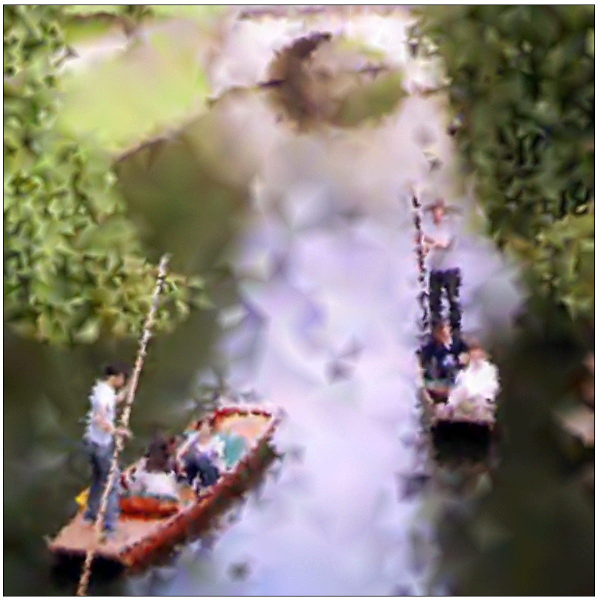

Gouraud shading:
linear interpolation of edges,
linear interpolation of interior.

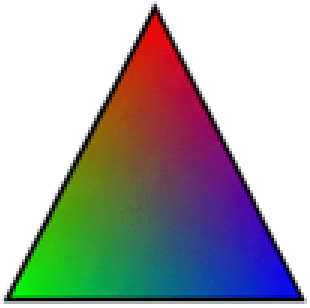

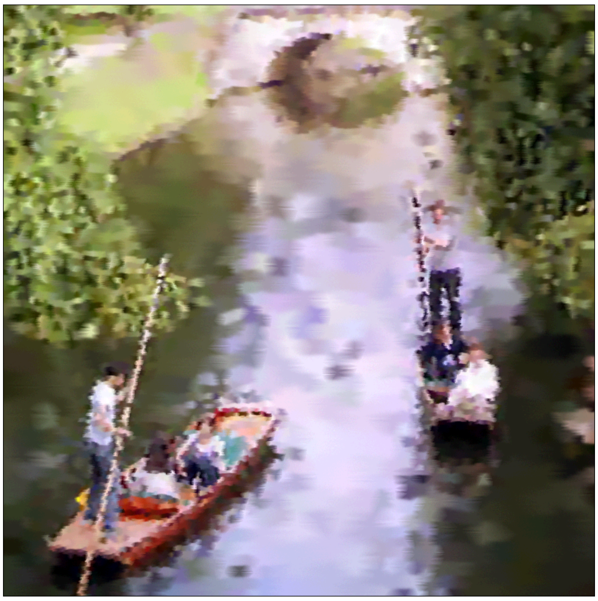

"Brush marks" rendering style:
nonlinear interpolation of edges,
linear interpolation of interior.

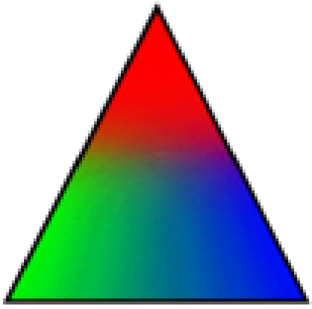

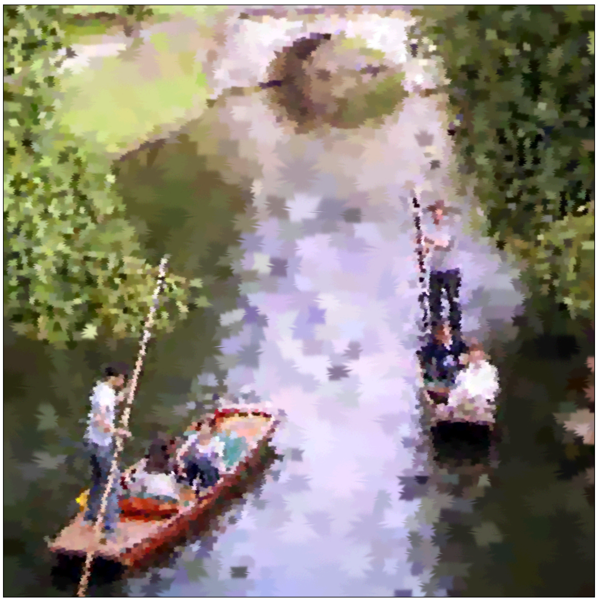

"Patchwork" rendering style:
nonlinear interpolation of edges,
nonlinear interpolation of interior.

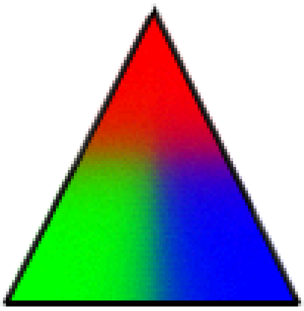

Figure 25: Basic geometric styles using importance driven coverage adaptive sampling (4800 samples ≈ 3%).

“Oil painting” geometric rendering style
(6400 samples ≈ 4%)

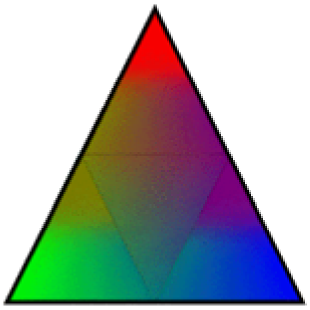

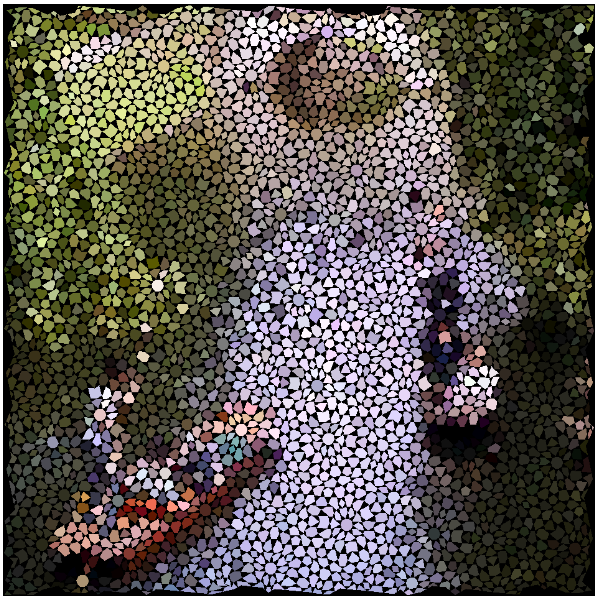

“Mosaic” geometric rendering style
(3200 samples ≈ 2%)

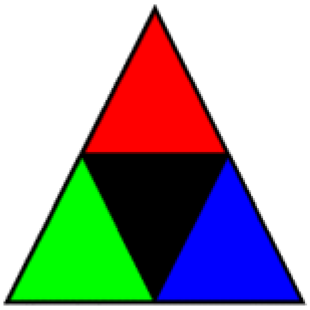

“Cubic strokes” geometric rendering style
(1600 samples ≈ 1%)

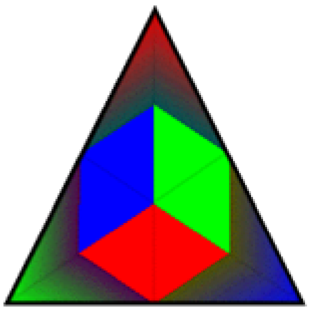

Figure 26: Design of geometric rendering styles applied using non-periodic quasicrystal sampling.

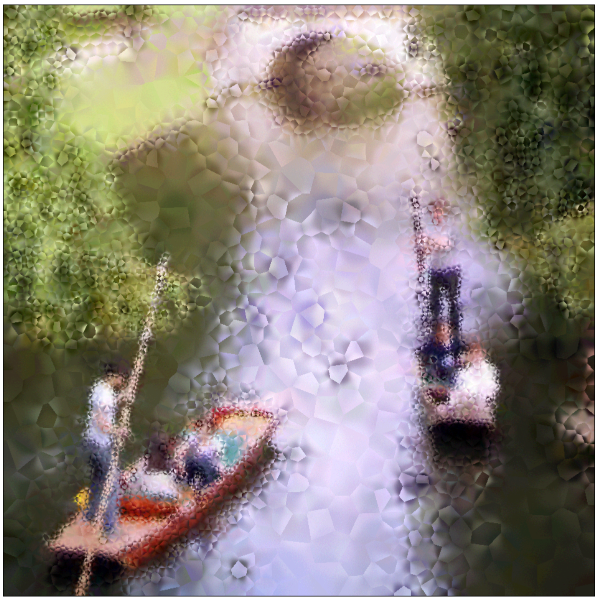

"Color facets" procedural rendering style
(4800 samples ≈ 3%)

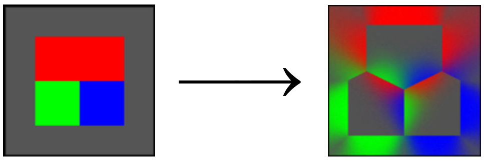

$$\phi(p,s_k)=\begin{cases}0 & \text{for } k=1\\ \Delta_2(p,s_k)^{-\alpha} & \text{for } k\neq 1\end{cases}$$

$$\Delta_\rho(p,s)=\sqrt[\rho]{\left|x_p-x_s\right|^\rho+\left|y_p-y_s\right|^\rho}$$

$$\Delta_2(p,s)=\sqrt{\left(x_p-x_s\right)^2+\left(y_p-y_s\right)^2}$$

$$\Delta_1(p,s)=\left|x_p-x_s\right|+\left|y_p-y_s\right|$$

parameter: $\alpha=6$

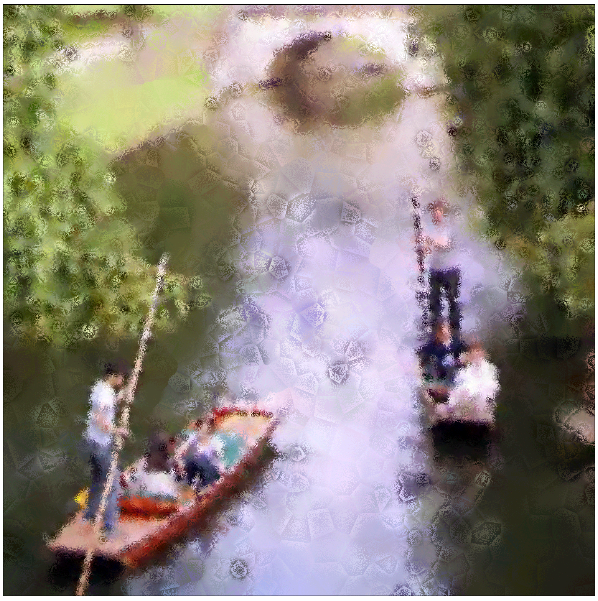

"Sponge painting" procedural rendering style
(4800 samples ≈ 3%)

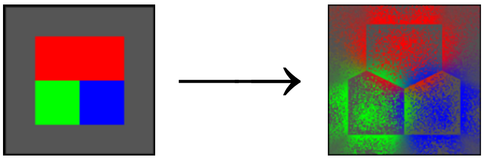

$$\phi(p,s_k)=\begin{cases}1 & \text{for } \delta\leq\xi,\ k=1\\ 0 & \text{for } \delta\leq\xi,\ k\neq 1\\ 0 & \text{for } \delta>\xi,\ k=1\\ \Delta_2(p,s_k)^{-\alpha} & \text{for } \delta>\xi,\ k\neq 1\end{cases}$$

$$\delta=\left(\frac{\Delta_2(p,s_1)}{\Delta_2(p,s_2)}\right)^{\frac{1}{\beta}} \quad \text{and} \quad \xi\sim\text{Uniform}[0,1]$$

parameters: $\alpha=6$ and $\beta=3$

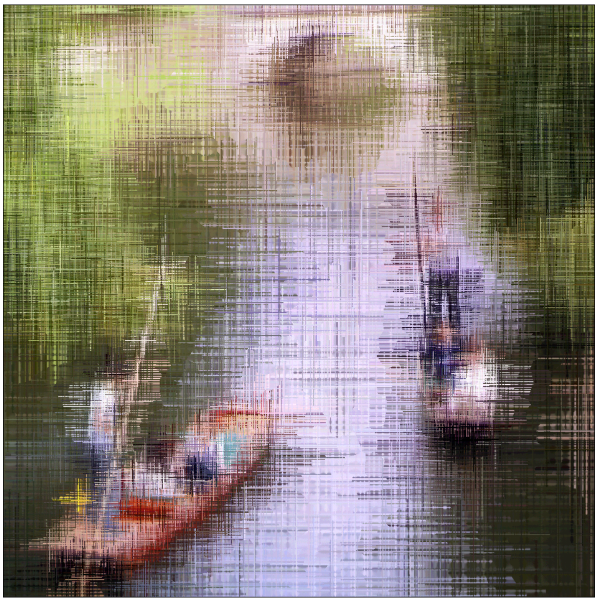

"Color hatching" procedural rendering style
(9600 samples ≈ 6%)

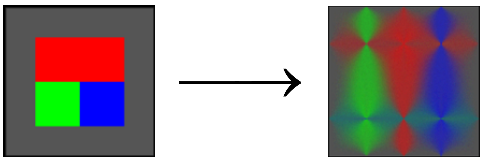

$$\phi(p,s_k)=\left|(1+\varepsilon)\Delta_1(p,s_k)-\Delta_2(p,s_k)\right|^{-\alpha}$$

parameters: $\alpha=3$ and small $\varepsilon=10^{-13}$

Figure 27: Design of procedural rendering styles applied using importance driven coverage adaptive sampling.

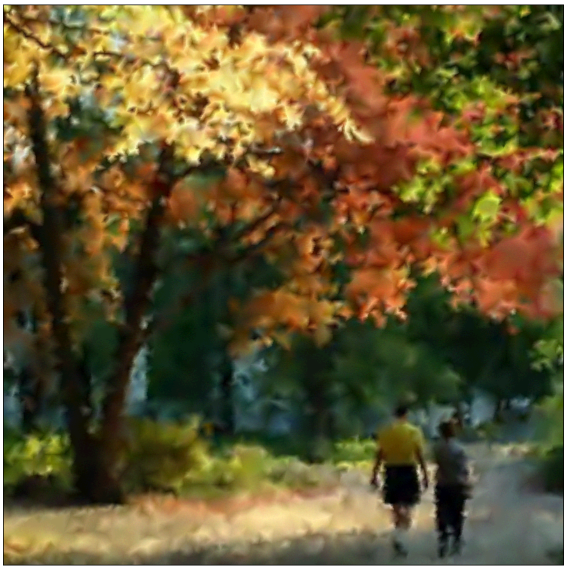

Gouraud shading

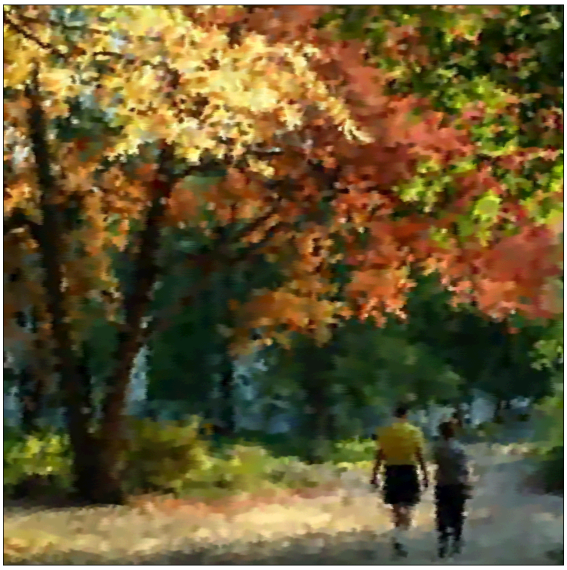

“Brush marks” geometric rendering style

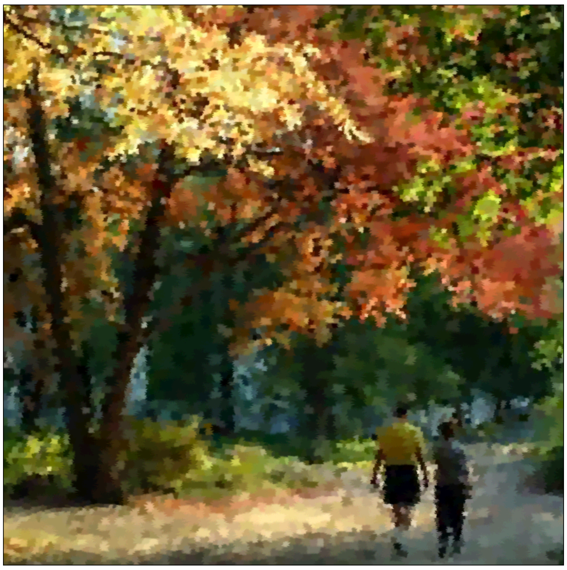

“Patchwork” geometric rendering style

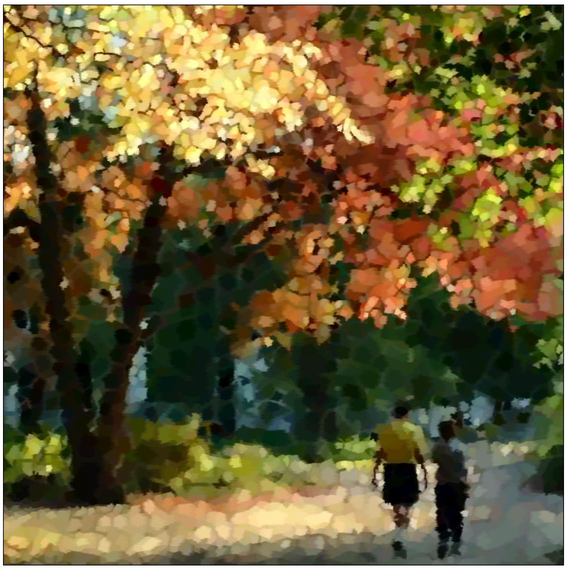

“Paint strokes” geometric rendering style

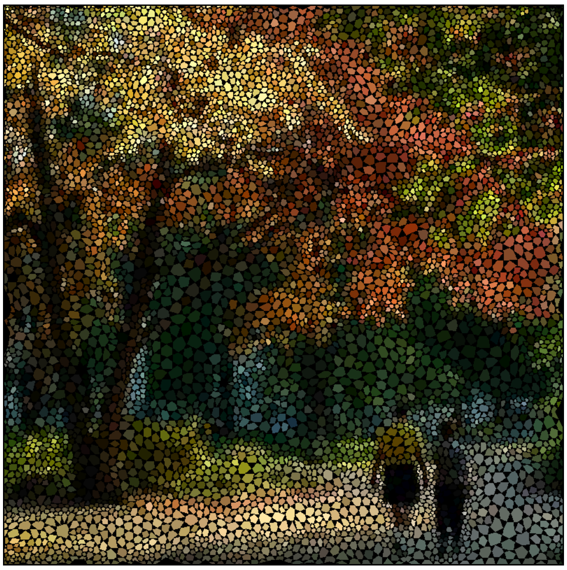

“Mosaic” geometric rendering style

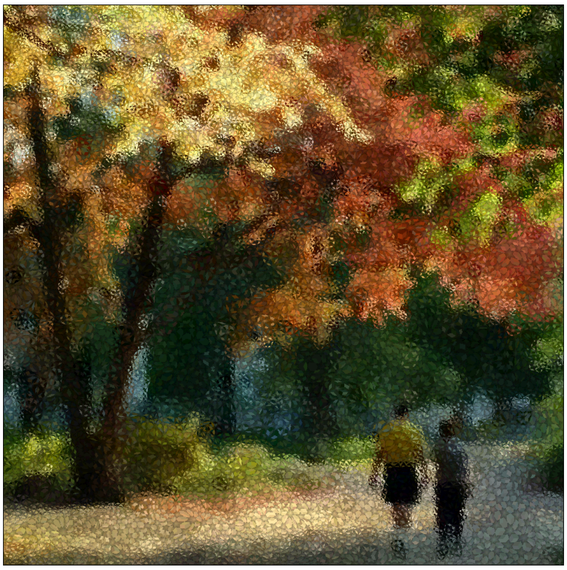

“Cubic strokes” geometric rendering style

Figure 28: Geometric rendering styles applied using coverage adaptive sampling (8000 samples ≈ 5%).

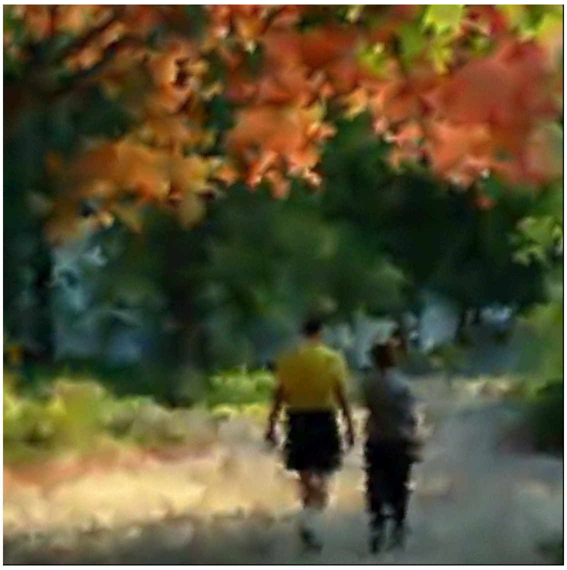
Gouraud shading

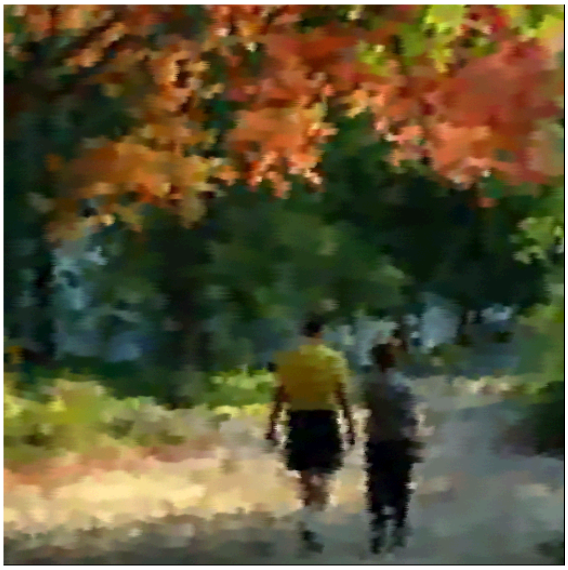
“Brush marks” geometric rendering style

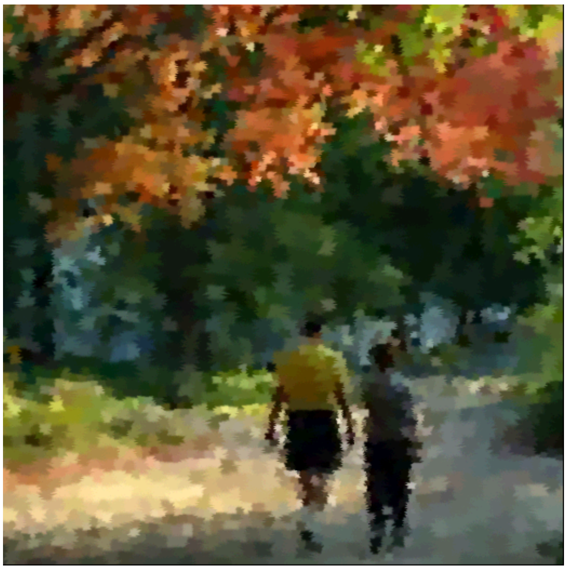
“Patchwork” geometric rendering style

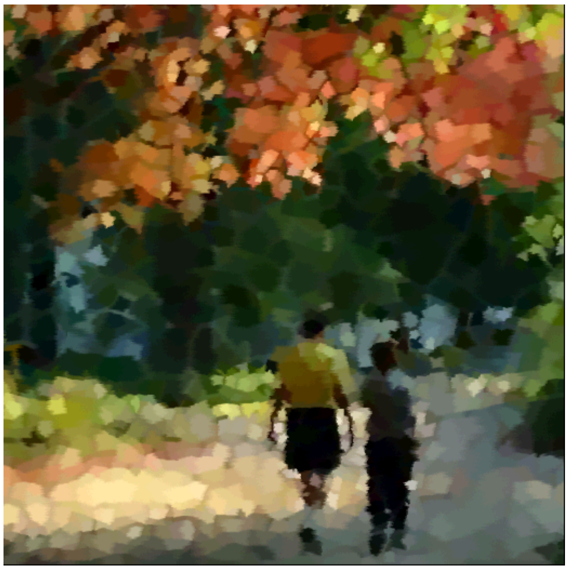
“Paint strokes” geometric rendering style

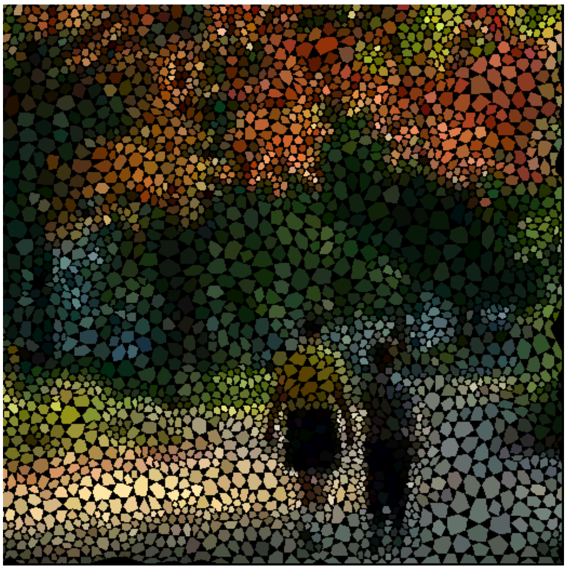
“Mosaic” geometric rendering style

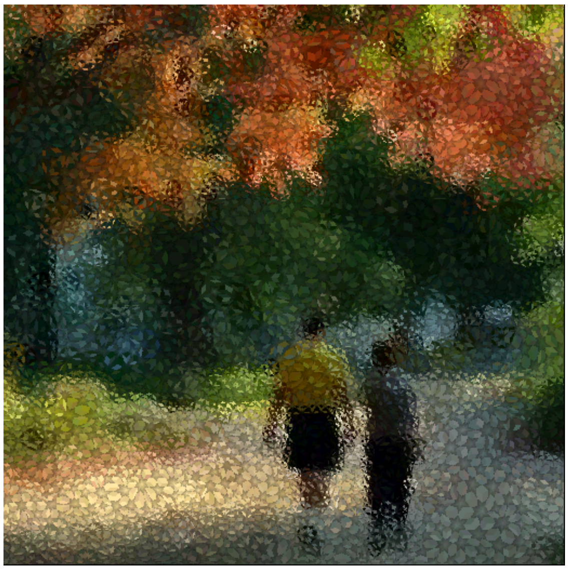
“Cubic strokes” geometric rendering style

Figure 29: Close-ups of geometric rendering styles applied using coverage adaptive sampling.

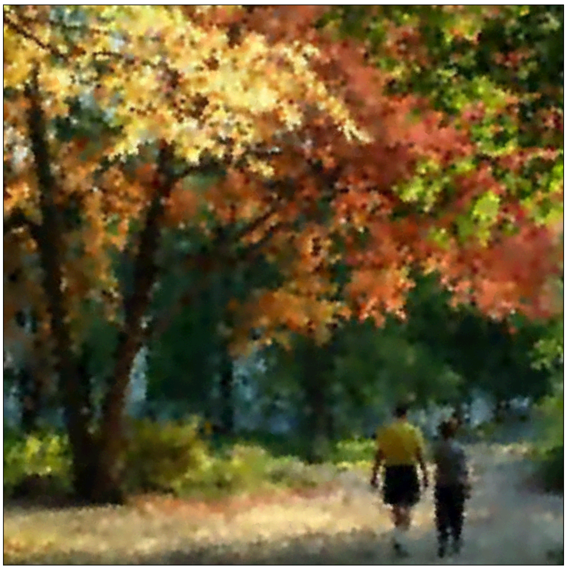

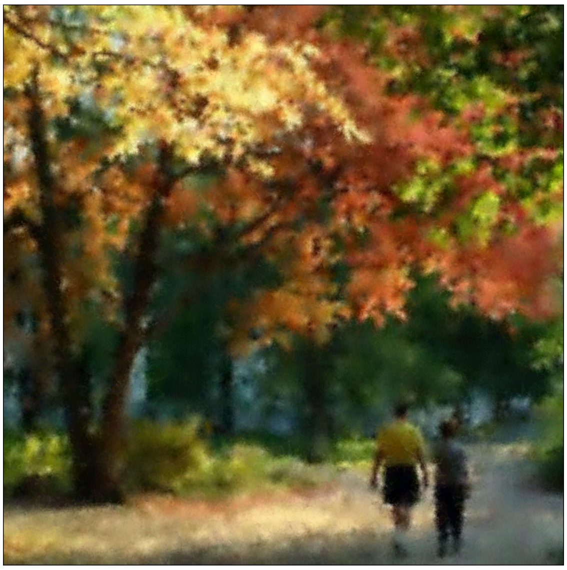

Shepard interpolation | "Soft touch" procedural rendering style

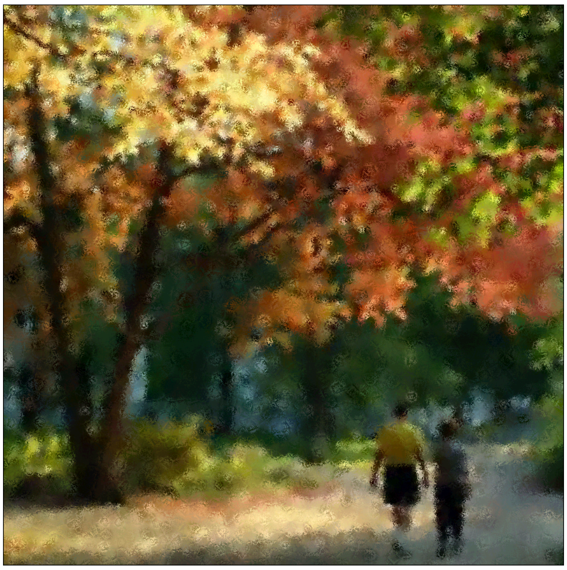

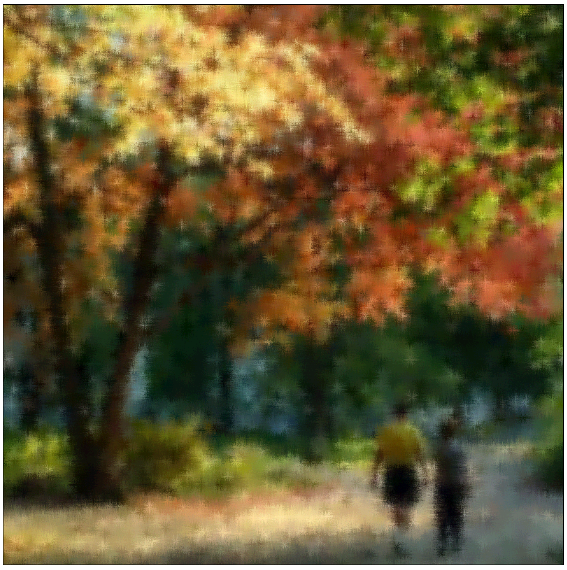

"Sponge painting" procedural rendering style | "Chalk painting" procedural rendering style

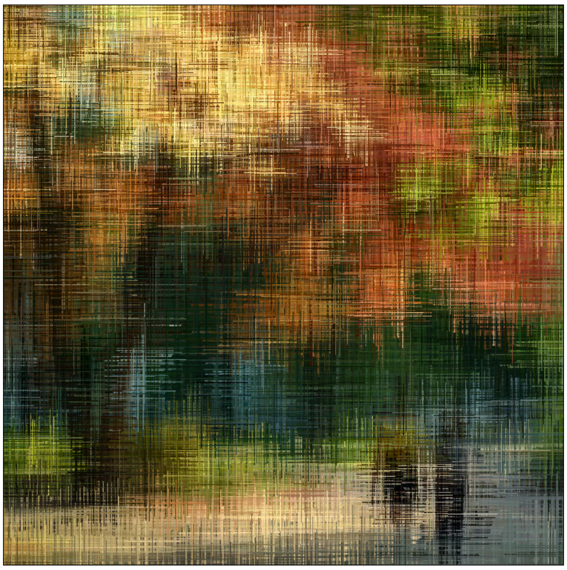

"Color hatching" procedural rendering style | "Ripple smoothing" procedural rendering style

Figure 30: Procedural rendering styles applied using coverage adaptive sampling (8000 samples $\approx$ 5%).

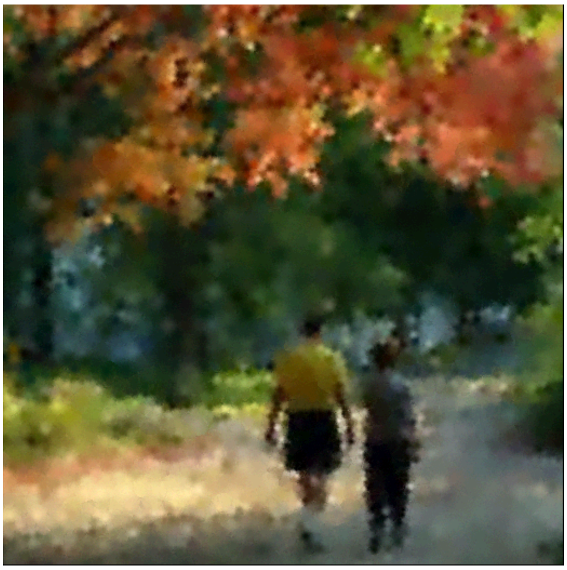
Shepard interpolation

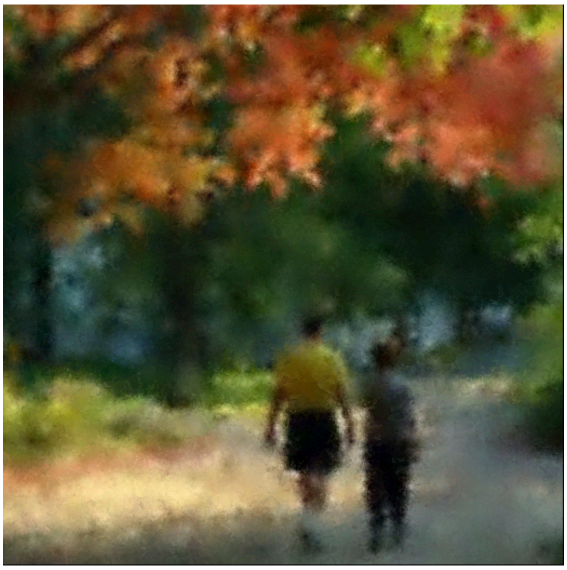
“Soft touch” procedural rendering style

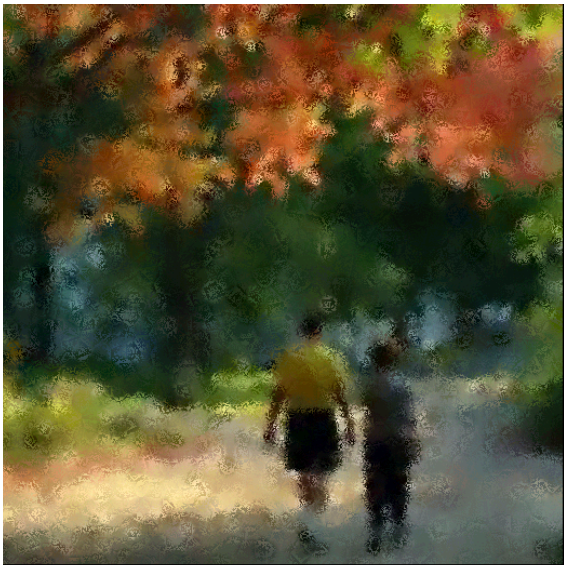
“Sponge painting” procedural rendering style

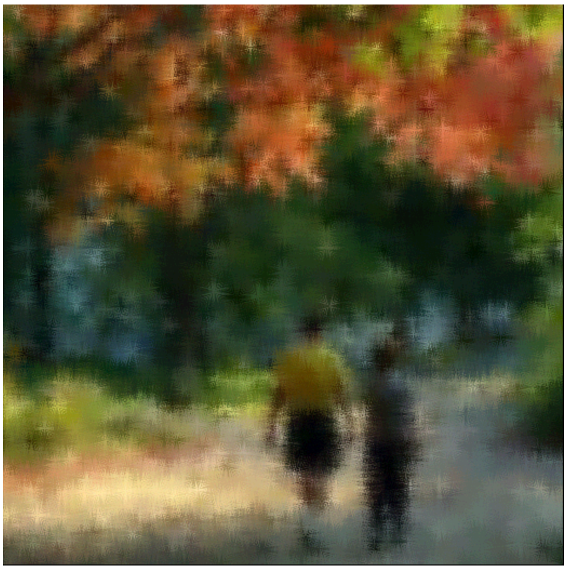
“Chalk painting” procedural rendering style

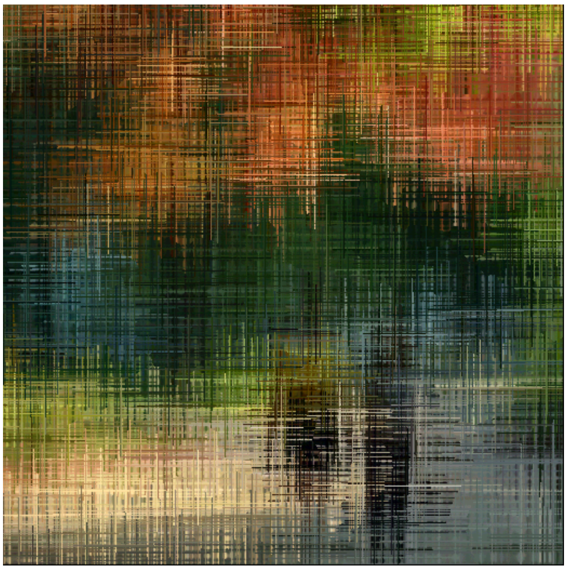
“Color hatching” procedural rendering style


“Ripple smoothing” procedural rendering style

Figure 31: Close-ups of procedural rendering styles applied using coverage adaptive sampling.

Coverage adaptive sampling with λ = 0.25

Coverage adaptive sampling with λ = 0.05

Figure 32: Adjusting the tradeoff between coverage and precision in coverage adaptive sampling rendered using the “paint strokes” geometric rendering style (6400 samples ≈ 4%).

Importance driven coverage adaptive sampling
(800 samples ≈ 0.5%)

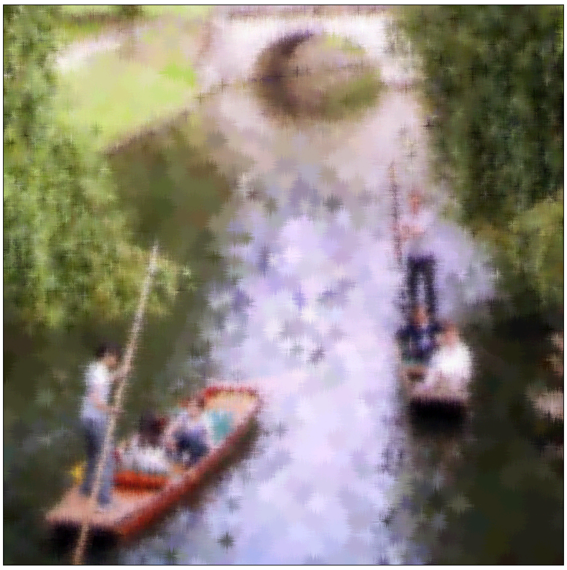

Importance driven coverage adaptive sampling
(8000 samples ≈ 5%)

Figure 33: Sampling density affects the look of the “chalk” procedural rendering style.

Figure 34: From figurative to abstract, interactively evolved rendering styles applied using jittered sampling.

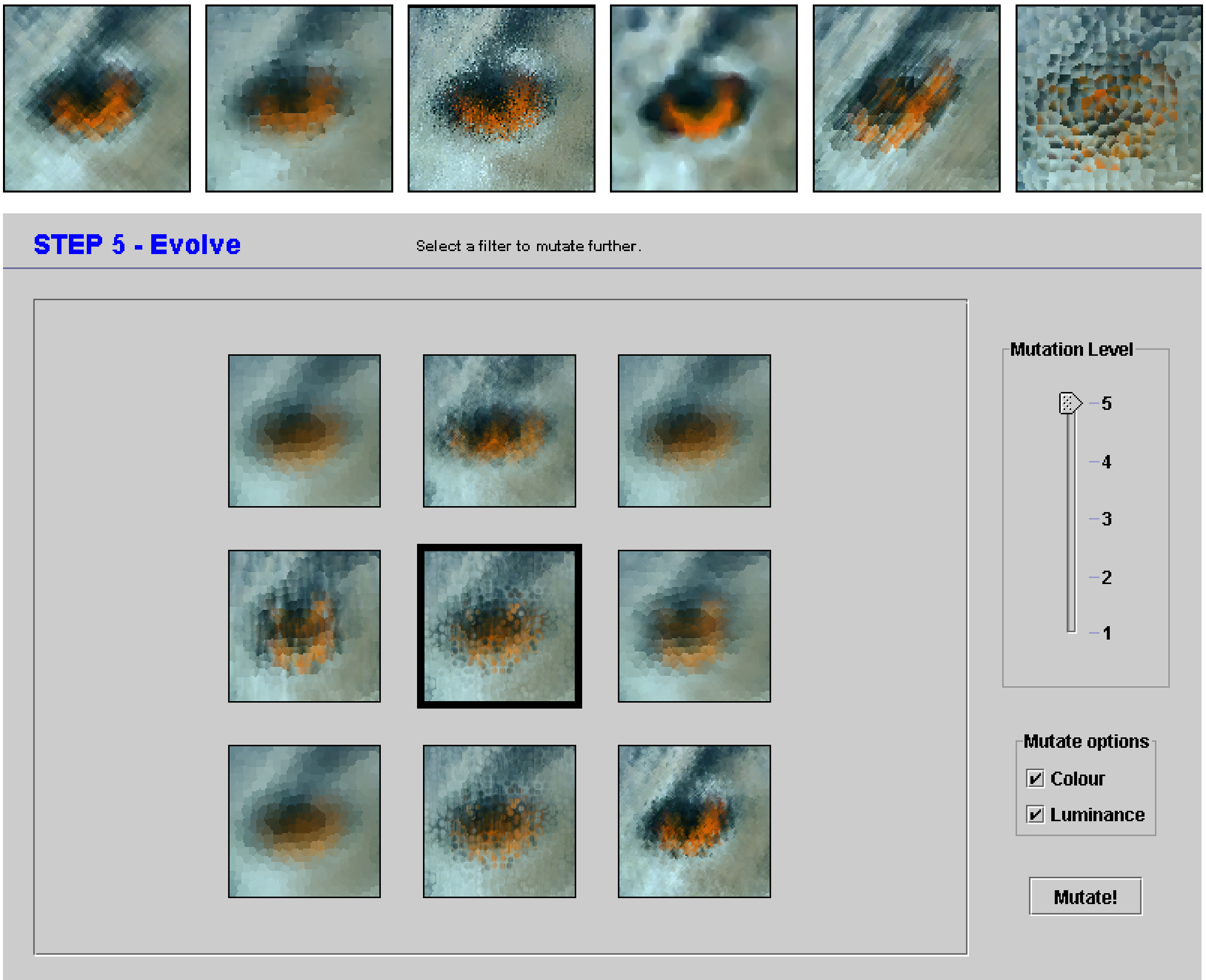

Figure 35: User interface for interactive evolution by aesthetic selection, with evolved styles shown above.

Figure 36: More interactively evolved rendering styles applied using jittered sampling.

Progressive rasterization by coloring the square tiles
produced using periodic square grid sampling:
1%, 2%, 4%, 8%, 16%, and 32%

Progressive rendering with the "paint strokes" style
applied using coverage adaptive sampling:
1%, 2%, 4%, 8%, 16%, and 32%

Figure 37: Comparison of photorealistic and non-photorealistic progressive rendering.

1000 samples ≈ 0.06%

2000 samples ≈ 1.25%

4000 samples ≈ 2.50%

8000 samples ≈ 5.00%

16000 samples ≈ 10.00%

32000 samples ≈ 20.00%

Figure 38: Progressive rendering with the “oil painting” style applied using quasirandom sampling.

“Lena” (512 × 512, 16-bit color)

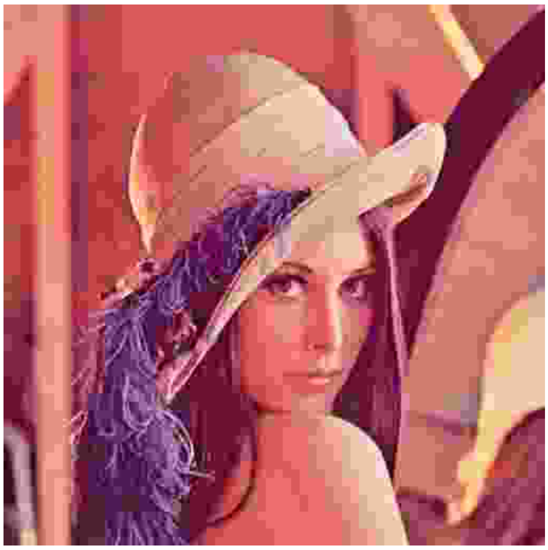

Standard JPEG compression (7.0K at 73:1)

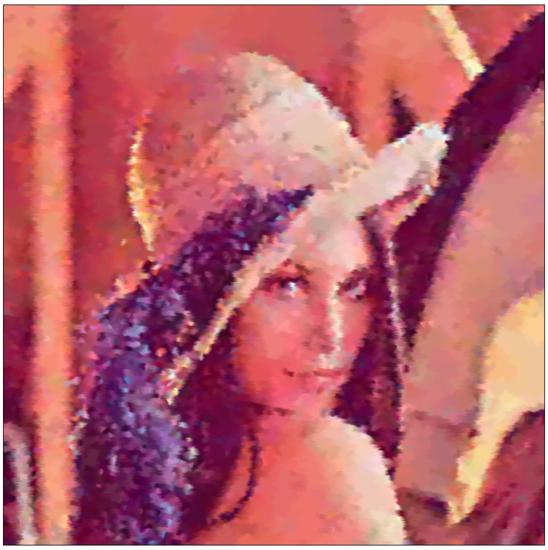

Our lossy compression rendered
using quasirandom sampling (6.1K at 84:1)

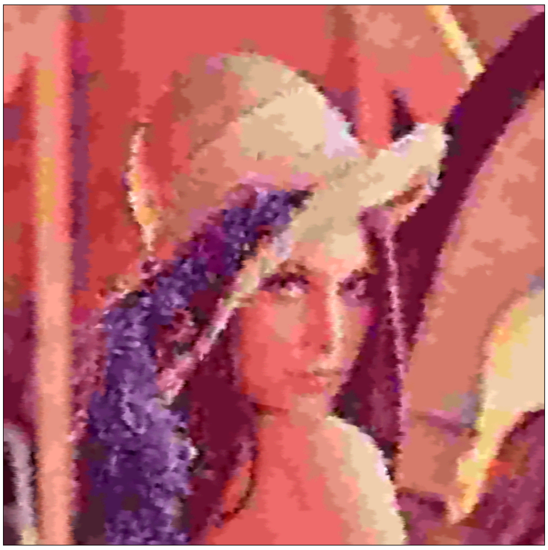

Standard JPEG compression rendered
using quasirandom sampling (7.0K at 73:1)

Our lossless compression rendered
using quasirandom sampling (12.8K at 40:1)

Our lossy compression rendered
using coverage adaptive sampling (7.2K at 71:1)

Figure 39: Image compression rendered with the “brush marks” style (10485 samples ≈ 4%).

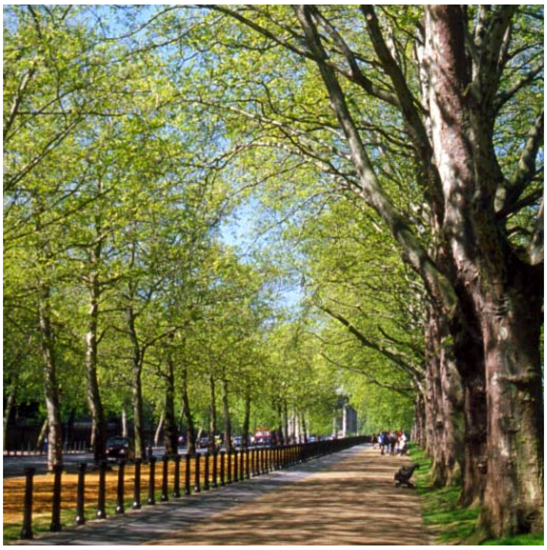

"Park" (512 × 512, 16-bit color)

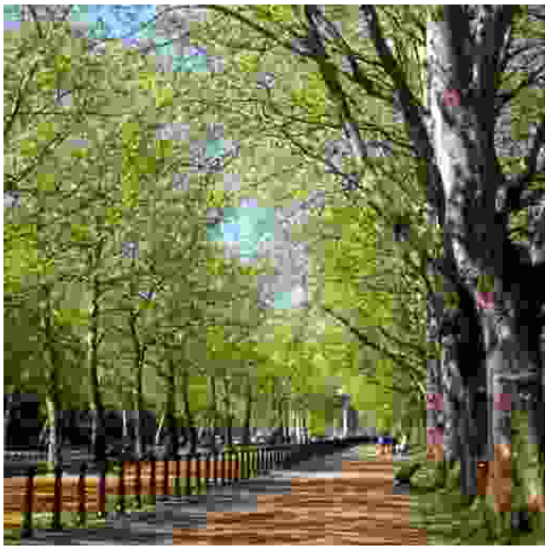

Standard JPEG compression (9.7K at 53:1)

Our lossy compression rendered
using quasirandom sampling (8.2K at 63:1)

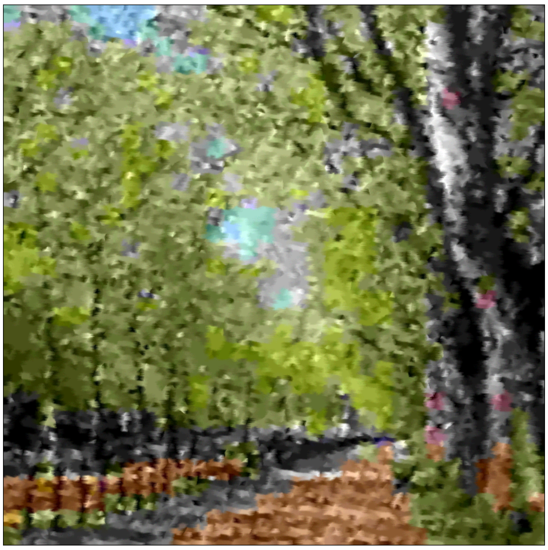

Standard JPEG compression rendered
using quasirandom sampling (9.7K at 53:1)

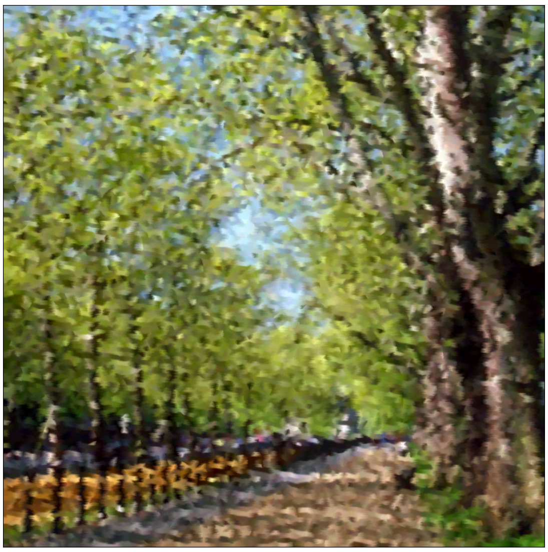

Our lossless compression rendered
using quasirandom sampling (17.5K at 29:1)

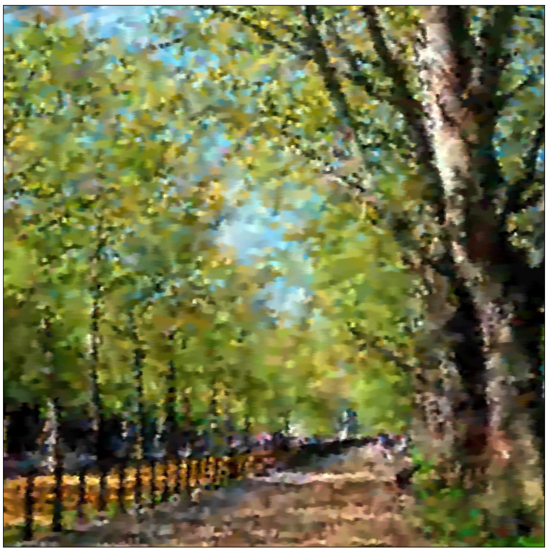

Our lossy compression rendered
using coverage adaptive sampling (8.5K at 60:1)

Figure 40: More image compression rendered with the "brush marks" style (10485 samples ≈ 4%).

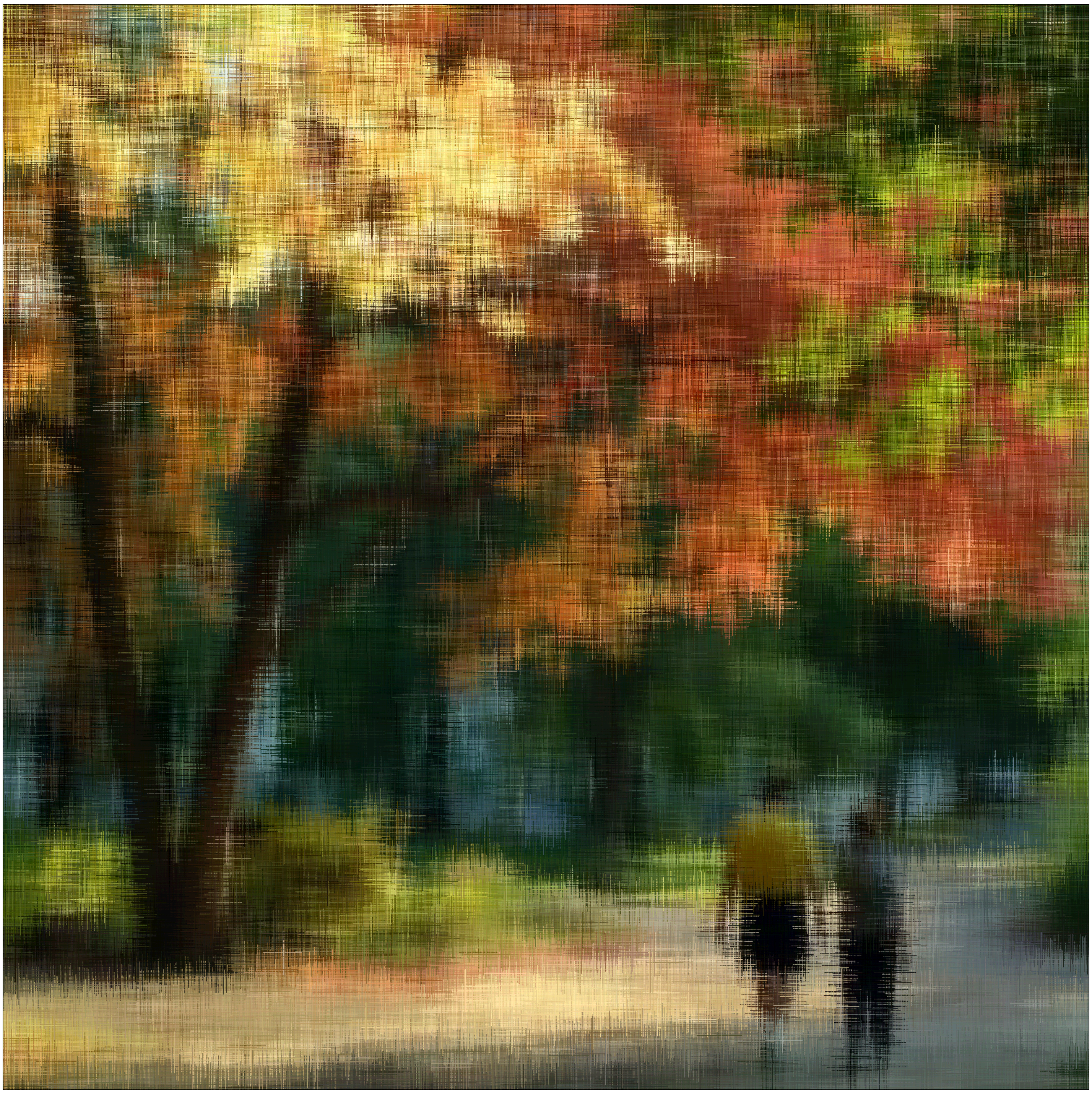

Figure 41: Non-photorealistic image rendering using the “color hatching” style with farthest point sampling (40000 samples ≈ 25%).